

Simulating pandemics with Agent-based Models

<http://www.prokopenko.net/SimPanABM.html>

Prof. Mikhail Prokopenko & Dr. Sheryl L. Chang
Centre for Complex Systems
School of Computer Science, Faculty of Engineering
Sydney Institute for Infectious Diseases



THE UNIVERSITY OF
SYDNEY

Tutorial, ALIFE 2022
20 July 2022



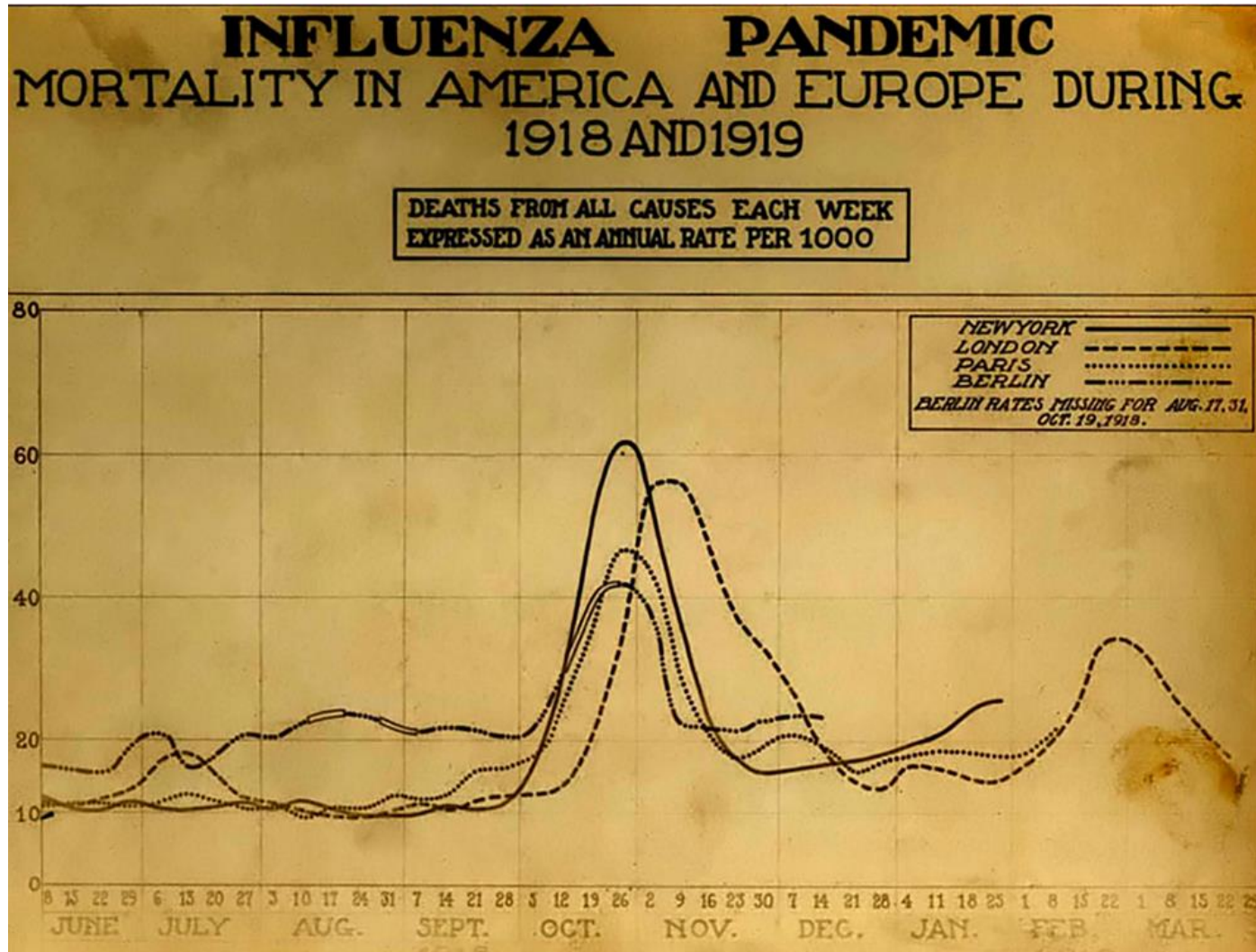
Spanish Flu 1918: 500 million infected, with deaths of three to five percent of the world's population



Soldiers from Fort Riley, Kansas, ill with Spanish influenza at a hospital ward at Camp Funston
Otis Historical Archives Nat'l Museum of Health & Medicine - NCP 1603



Spanish Flu 1918: a chart of deaths in major cities



Pandemic Influenza: The Inside Story. Nicholls H, *PLoS Biology* Vol. 4/2/2006, e50
courtesy of the National Museum of Health and Medicine



“I had hoped that hitting the 100th anniversary of this epidemic (Spanish flu) would spark a lot of discussion about whether we’re ready for the next global epidemic. Unfortunately, it didn't, and we still are not ready”

Bill Gates
Chair of Bill & Melinda Gates Foundation
2018

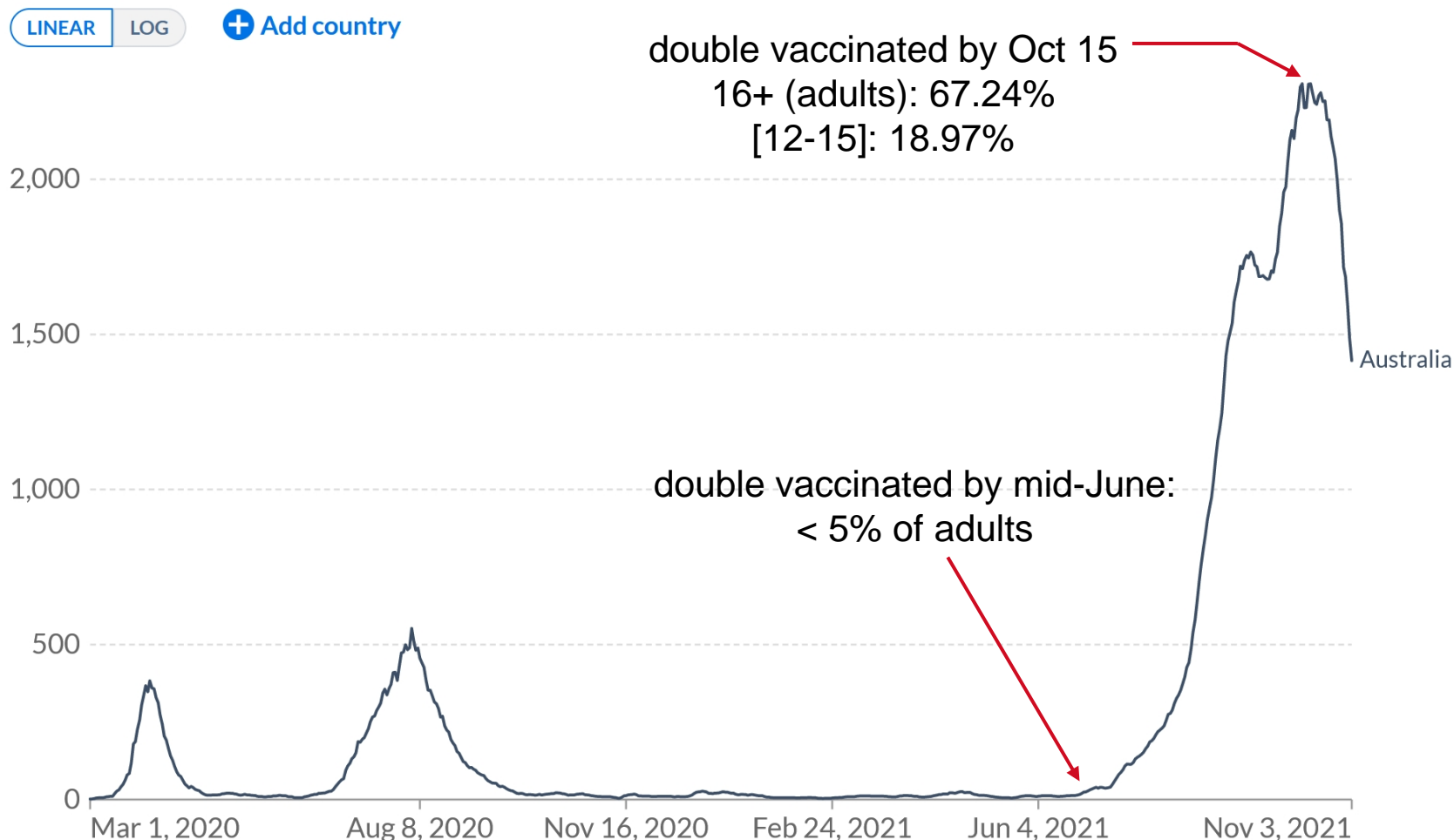


The Delta variant: 3rd pandemic wave in Australia (November 3, 2021)

Daily new confirmed COVID-19 cases

7-day rolling average. Due to limited testing, the number of confirmed cases is lower than the true number of infections.

Our World
in Data





THE UNIVERSITY OF
SYDNEY

The Omicron variant: 4th pandemic wave in Australia (July 16, 2022)

Our World
in Data

Daily new confirmed COVID-19 cases per million people

7-day rolling average. Due to limited testing, the number of confirmed cases is lower than the true number of infections.

LINEAR

LOG



Source: Johns Hopkins University CSSE COVID-19 Data

CC BY

► Jan 31, 2020



Jul 15, 2022

A Contribution to the Mathematical Theory of Epidemics.

By W. O. KERMACK and A. G. McKENDRICK.

(Communicated by Sir Gilbert Walker, F.R.S.—Received May 13, 1927.)

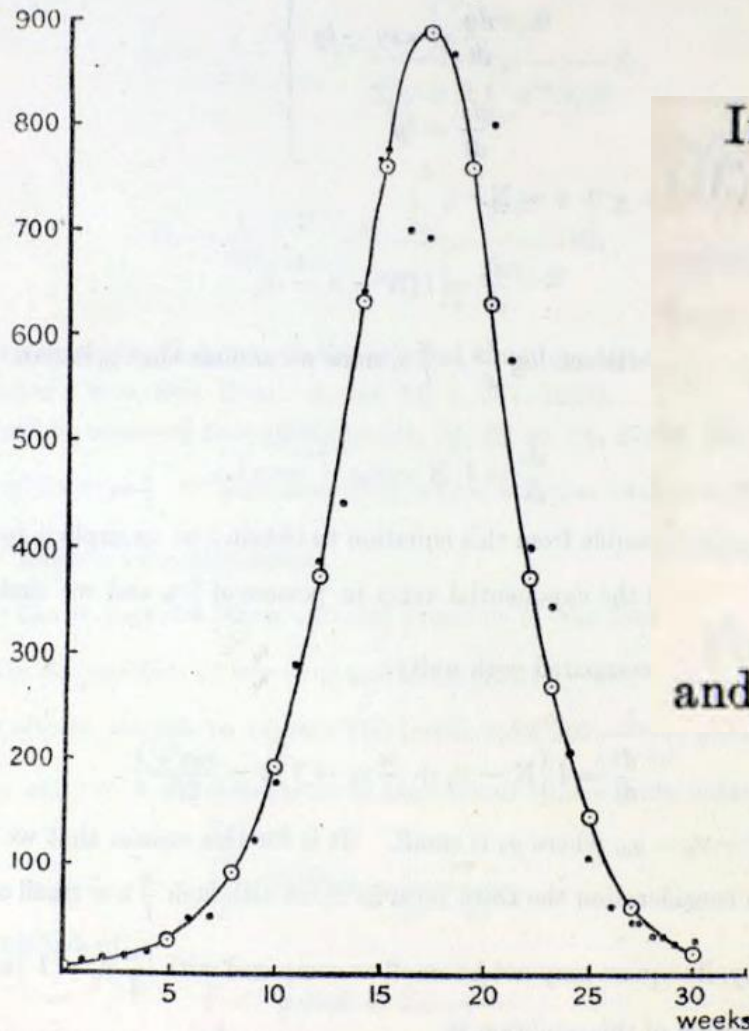
(From the Laboratory of the Royal College of Physicians, Edinburgh.)

Introduction.

(1) One of the most striking features in the study of epidemics is the difficulty of finding a causal factor which appears to be adequate to account for the magnitude of the frequent epidemics of disease which visit almost every population. It was with a view to obtaining more insight regarding the effects of the various factors which govern the spread of contagious epidemics that the present investigation was undertaken. Reference may here be made to the work of Ross



Compartmental models in epidemiology: Susceptible – Infectious – Recovered



The accompanying chart is based upon figures of deaths from plague in the island of Bombay over the period December 17, 1905, to July 21, 1906. The ordinate represents the number of deaths per week, and the abscissa denotes the time in weeks. As at least

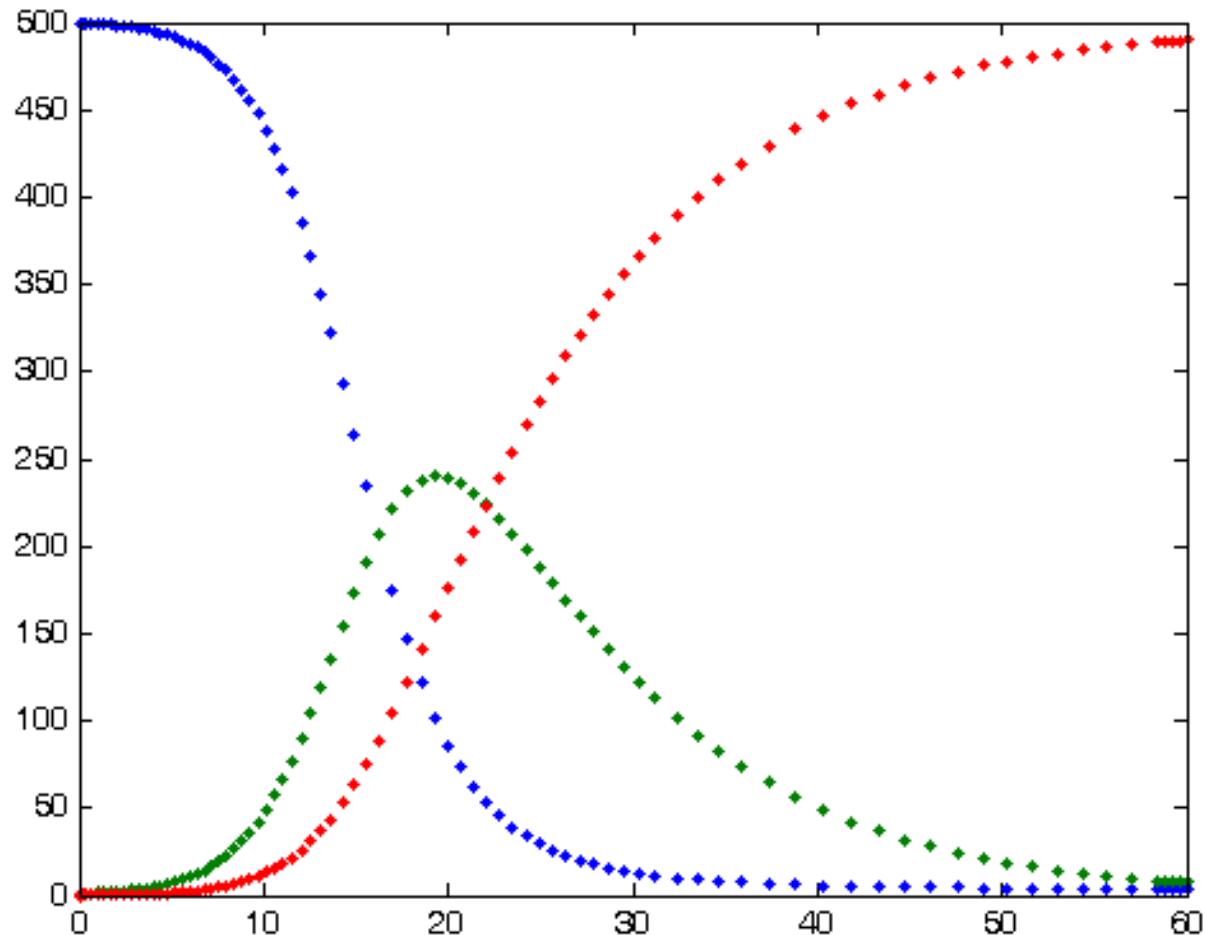
In this case the equations are

$$\left. \begin{aligned} \frac{dx}{dt} &= -\kappa xy \\ \frac{dy}{dt} &= \kappa xy - ly \\ \frac{dz}{dt} &= ly \end{aligned} \right\}$$

and as before $x + y + z = N$.



Compartmental models in epidemiology: Susceptible – Infectious – Recovered



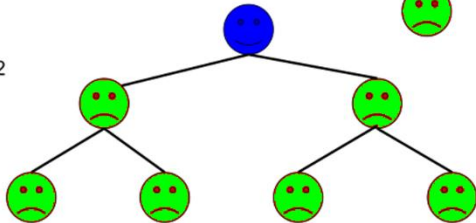


Epidemic modelling: reproductive ratio R_0

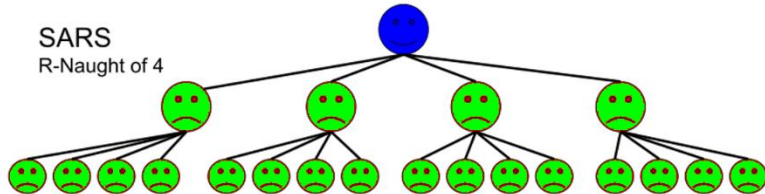
● Patient Zero

● Infected

Ebola:
R-Naught of 2



SARS
R-Naught of 4



$$\frac{dS}{dt} = \gamma I - \beta IS$$

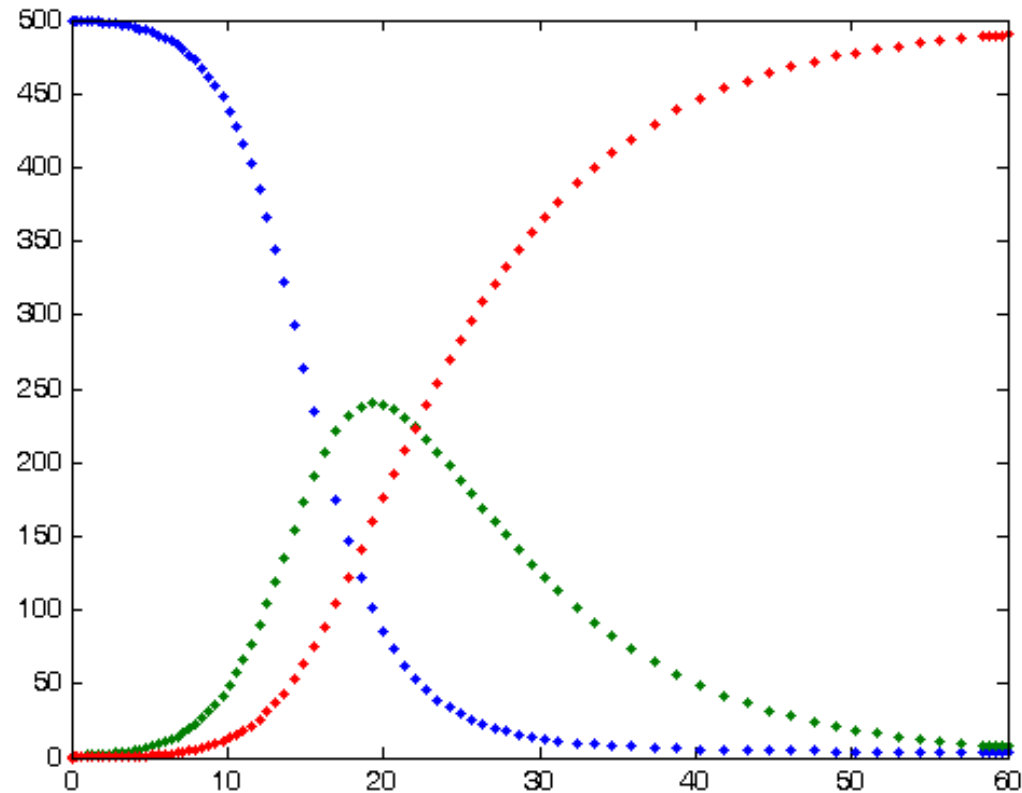
$$\beta / \gamma = R_0$$

$$\frac{dI}{dt} = \beta IS - \gamma I,$$

Susceptible

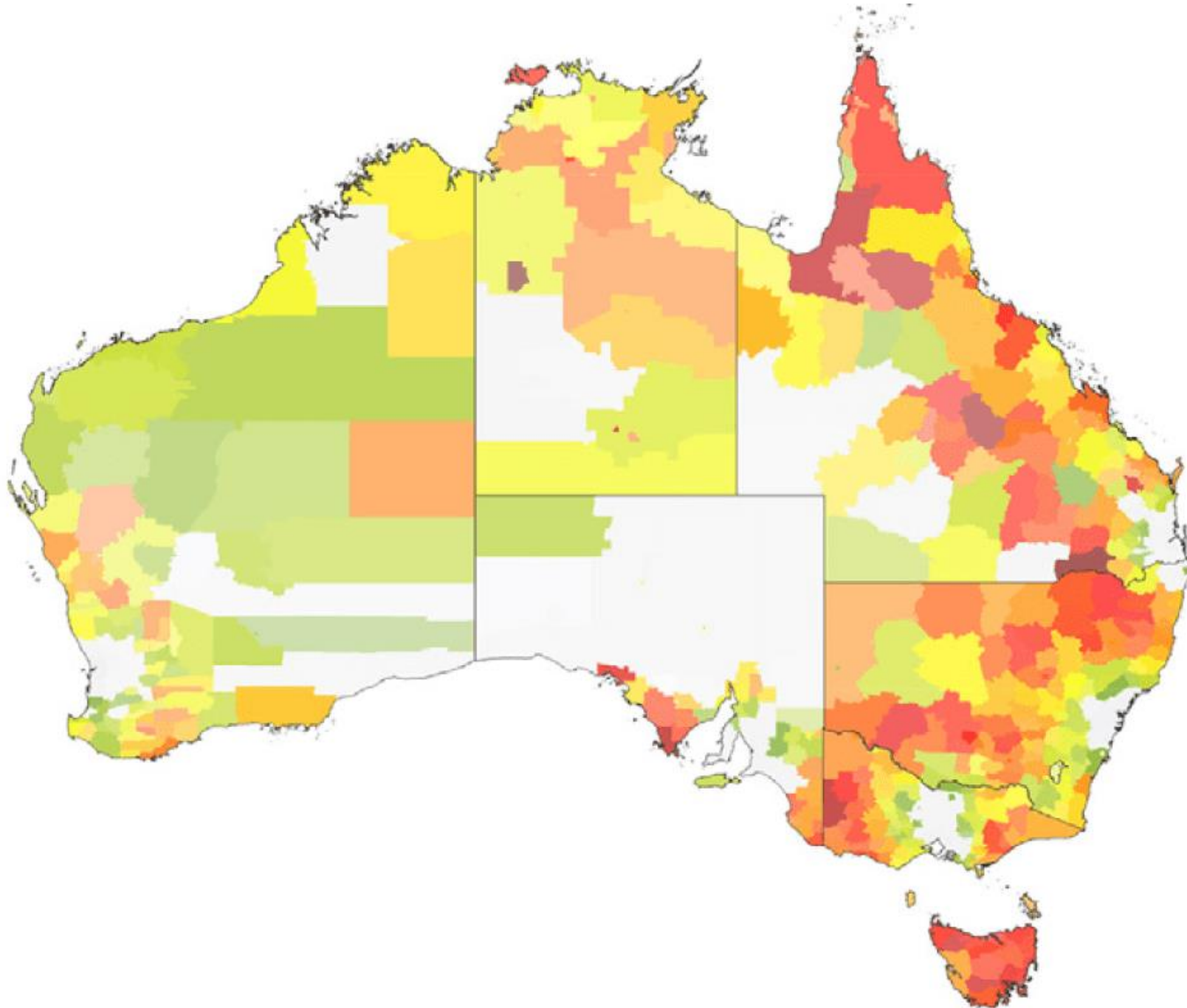
Infectious

Recovered



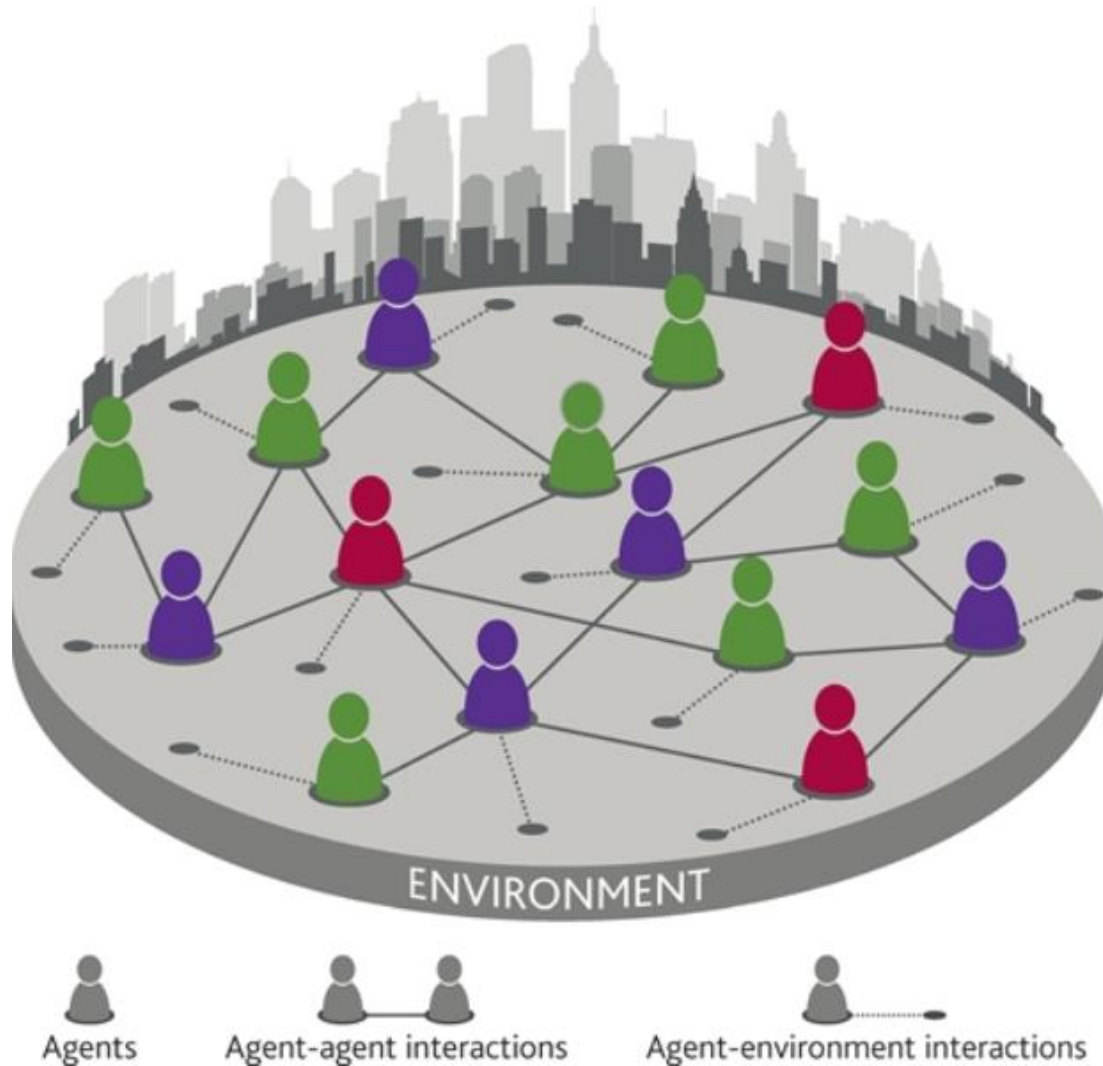


Different questions: How to “zoom in” ? Where / how to intervene?





Agent-based modelling (ABM)





THE UNIVERSITY OF
SYDNEY

A little bit more on history...

International Journal of Modern Physics C
Vol. 15, No. 1 (2004) 193–201
© World Scientific Publishing Company

 **World Scientific**
www.worldscientific.com

LARGE-SCALE MOLECULAR-DYNAMICS SIMULATION OF 19 BILLION PARTICLES

KAI KADAU

*Theoretical Division, Los Alamos National Laboratory
MS B262, Los Alamos, New Mexico 87545, USA
kkadau@lanl.gov*

TIMOTHY C. GERMANN

*Applied Physics Division, Los Alamos National Laboratory
MS F699, Los Alamos, New Mexico 87545, USA
tcg@lanl.gov*

PETER S. LOMDAHL

*Theoretical Division, Los Alamos National Laboratory
MS B262, Los Alamos, New Mexico 87545, USA
pxl@lanl.gov*

Received 8 August 2003
Revised 10 August 2003



SPaSM: Scalable Parallel Short-range Molecular dynamics

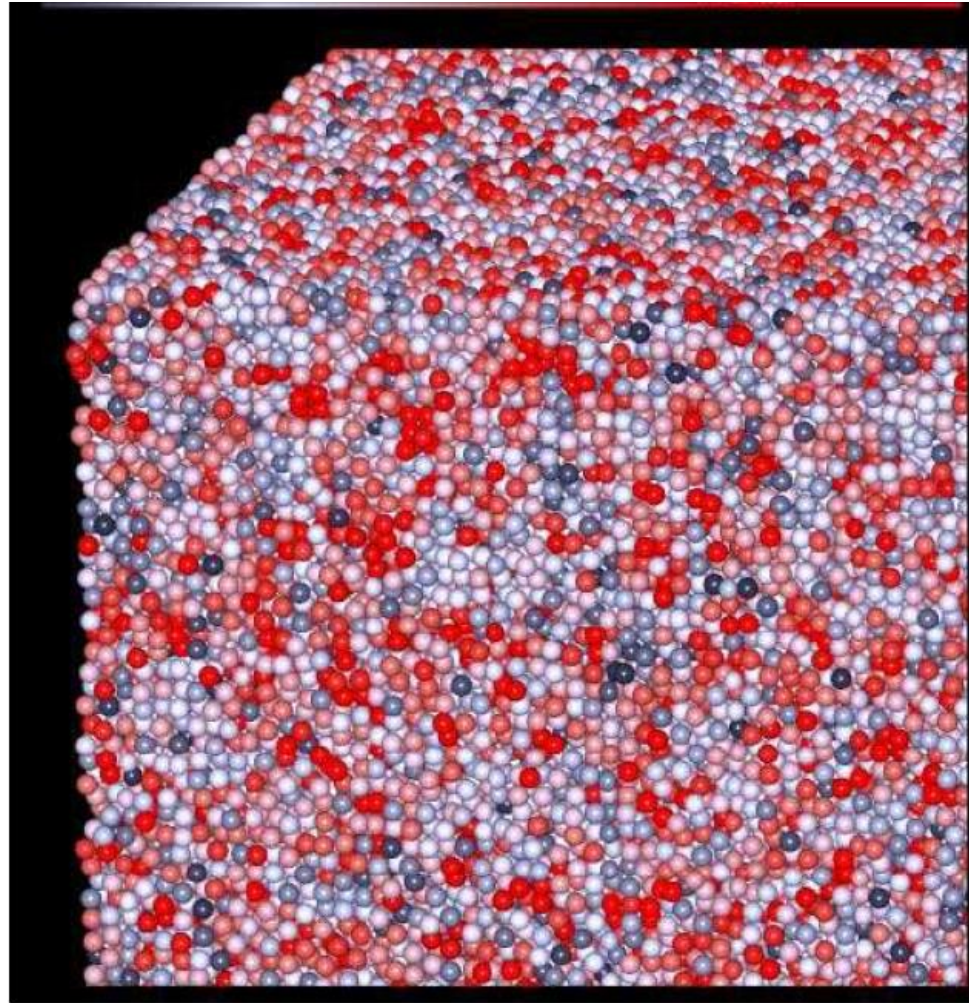


Fig. 3. ≈ 37 million particles rendered on four PN with a resolution of 5000 pixel by 5000 pixel (top). The bottom shows a close-up of the same picture file. The grayscale represents the potential energies of the atoms from -6 to -2 (grayscale version of the original color picture).



Mitigation strategies for pandemic influenza in the United States

Timothy C. Germann^{*†}, Kai Kadau^{*}, Ira M. Longini, Jr.[‡], and Catherine A. Macken^{*}

^{*}Los Alamos National Laboratory, Los Alamos, NM 87545; and [†]Program of Biostatistics and Biomathematics, Fred Hutchinson Cancer Research Center and Department of Biostatistics, School of Public Health and Community Medicine, University of Washington, Seattle, WA 98109

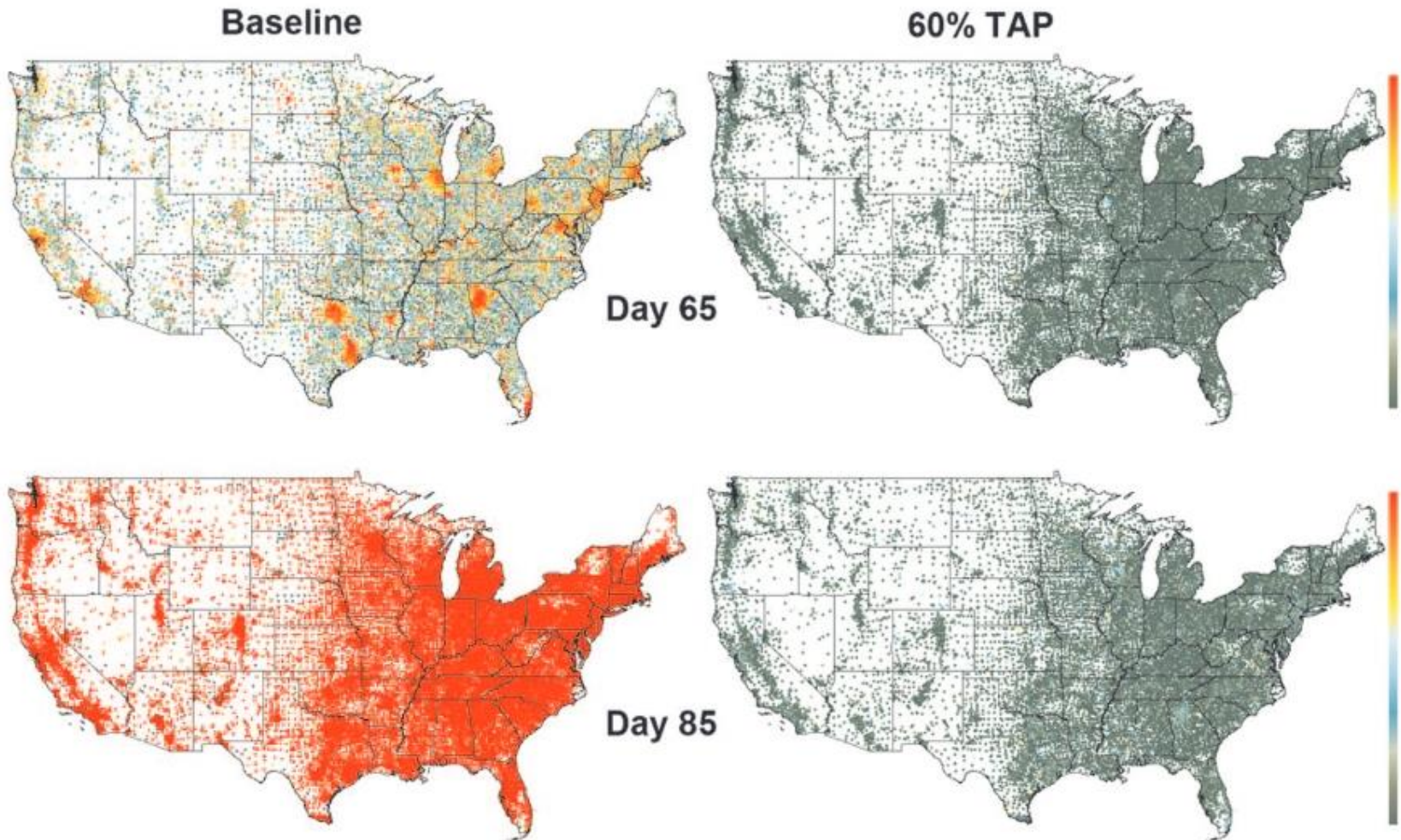
Communicated by G. Balakrish Nair, International Centre for Diarrhoeal Disease Research Bangladesh, Dhaka, Bangladesh, February 16, 2006
(received for review January 10, 2006)

Recent human deaths due to infection by highly pathogenic (H5N1) avian influenza A virus have raised the specter of a devastating pandemic like that of 1917–1918, should this avian virus evolve to become readily transmissible among humans. We introduce and use a large-scale stochastic simulation model to investigate the spread of a pandemic strain of influenza virus through the U.S. population of 281 million individuals for R_0 (the basic reproductive number) from 1.6 to 2.4. We model the impact that a variety of

resources to minimize the impact of the outbreak? Precise planning is hampered by several unknowns, most critically the eventual human-to-human transmissibility of the human-adapted avian strain (characterized by the basic reproductive number R_0 , the average number of secondary infections caused by a single typical infected individual among a completely susceptible population), and the supply of therapeutic agents. Manufacturers of neuraminidase inhibitors, such as oseltamivir,



Pandemic influenza: agent-based modelling (Germann et al., 2006)



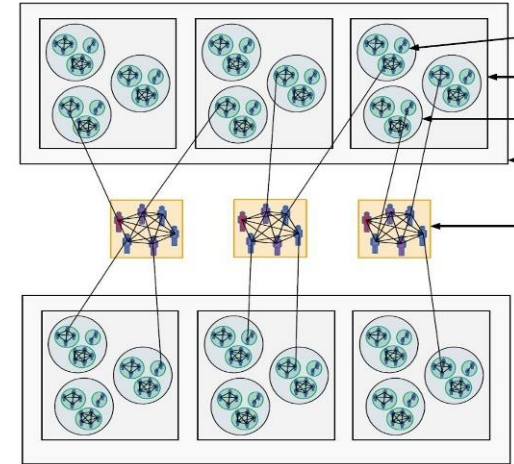
- Modelling pandemics with large-scale high-resolution agent-based models
 - *demographics*: from census based data to agents
 - *mobility*: travel patterns including long-distance
 - *infection*: disease transmission and natural history models
 - ACEMod – Australian Census-based Epidemic Model

- Influenza pandemics (H1N1):
 - pandemic trends (peaks, synchrony, bimodality, critical regimes)
 - effects of urbanisation
 - counter-factual analysis
 - efficiency of interventions: geographically-targeted anti-prophylaxis (GTAP), contact-targeted anti-prophylaxis (TAP), vaccination

Pandemic modelling using Agent-based Models

➤ Large-scale high-resolution agent-based models

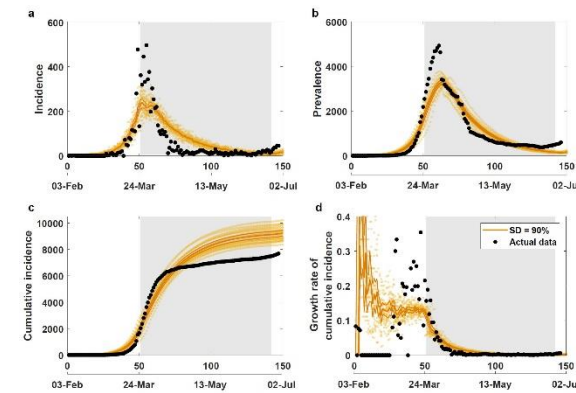
- *demographics*: from census based data to agents
- *mobility*: travel patterns including long-distance
- *infection*: epidemiology



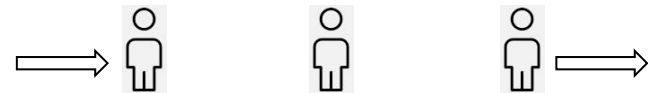
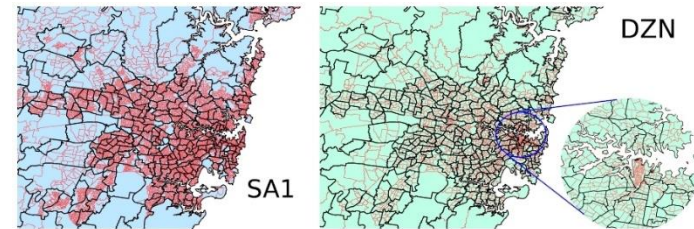
➤ AMTraC-19: Agent-based **M**odel of **T**ransmission and **C**ontrol of the COVID-19 pandemic in Australia (~ 24M agents)

➤ Model calibration and validation during COVID-19 pandemic

- first wave (Australia: March – June 2020)
- second wave (Victoria: July – September 2020)
- third wave (NSW / Australia: June – November 2021)



- ~24M stochastically generated agents (Census, ABS & ACARA data)
- household size and composition vary across different local areas
- commuting patterns between residence and work / study
- flexible infection seeding scenarios
- transmission within mixing contexts
- different symptomatic ratios for children and adults
- vaccination rollout with two vaccines
- vaccine efficacy split across components (infection, symptoms, transmission)
- varying social distancing (“stay-at-home” restrictions)

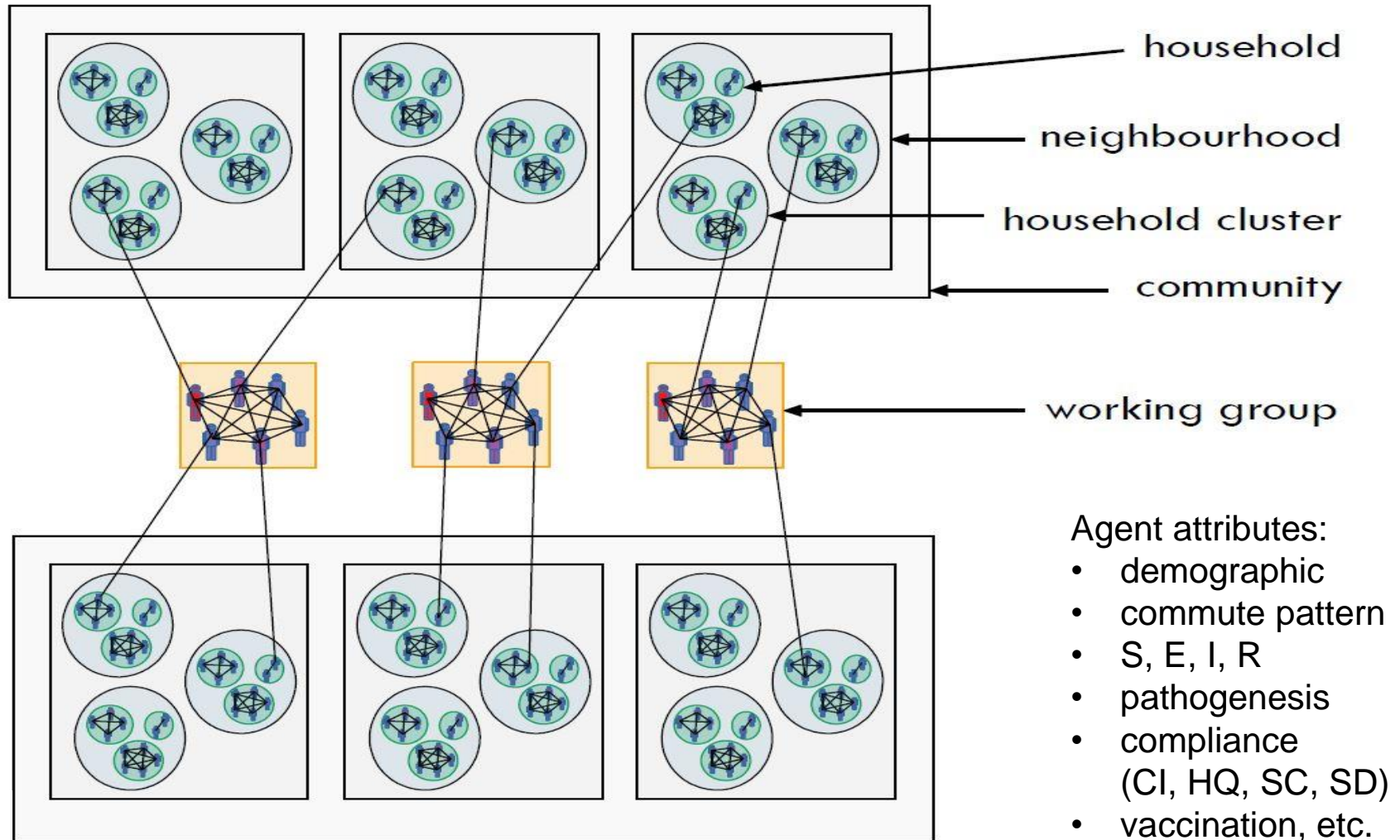


S. L. Chang, N. Harding, C. Zachreson, O. M. Cliff, M. Prokopenko, Modelling transmission and control of the COVID-19 pandemic in Australia, *Nature Communications*, 11, 5710, 2020.

C. Zachreson, S. L. Chang, O. M. Cliff, M. Prokopenko, How will mass-vaccination change COVID-19 lockdown requirements in Australia? *The Lancet Regional Health – Western Pacific*, 14: 100224, 2021.



“Same storm, different boats”: Agent-based Modelling



Population partitions: residential areas and destination zones

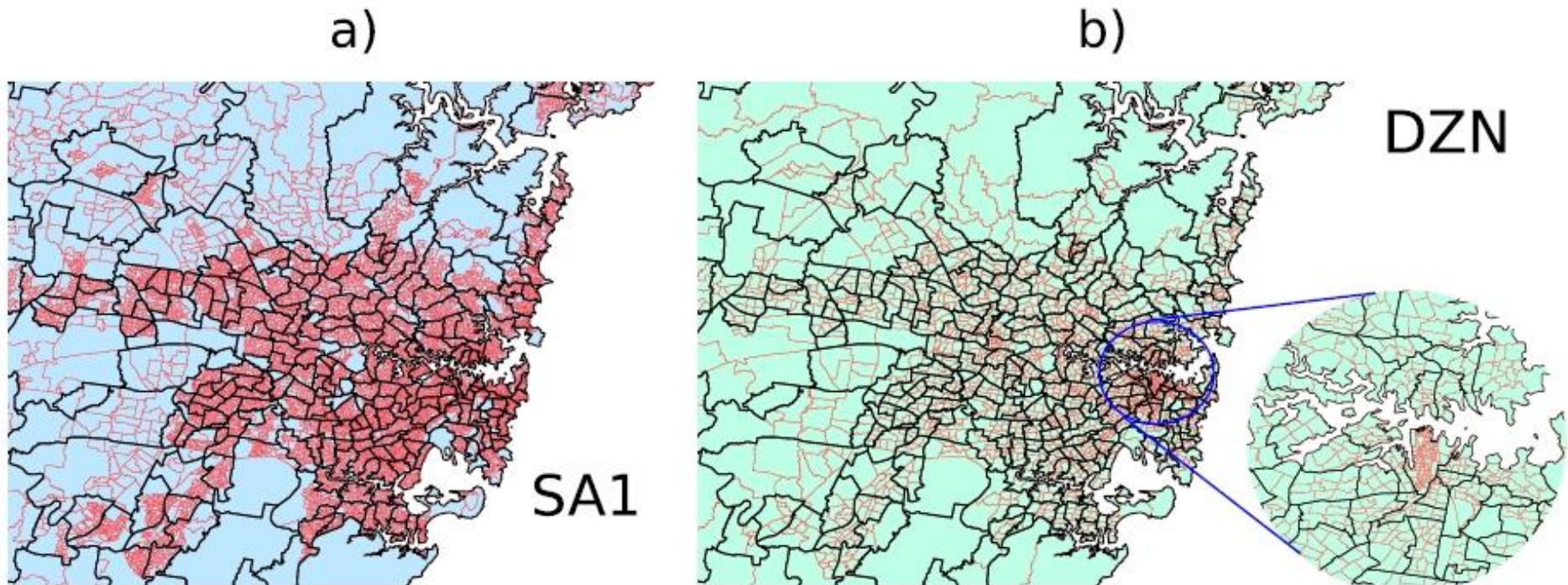


Fig. 1 Maps of the Greater Sydney region illustrating the distribution of population partitions. (a) A map of the Greater Sydney region showing SA2 (black) and SA1 (red) population partitions. (b) A map of the same area showing SA2 (black) and DZN (red) partitions. The inset in (b) zooms in on the Sydney central business district to illustrate the much denser packing of DZN partitions in that area.



THE UNIVERSITY OF
SYDNEY

Australian Census-based Epidemic Model: ACEMod

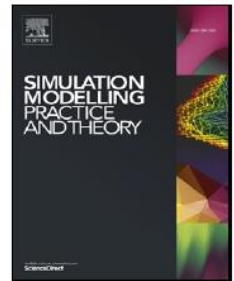
Simulation Modelling Practice and Theory 87 (2018) 412–431



Contents lists available at [ScienceDirect](#)

Simulation Modelling Practice and Theory

journal homepage: www.elsevier.com/locate/simpat



Investigating spatiotemporal dynamics and synchrony of influenza epidemics in Australia: An agent-based modelling approach



Oliver M. Cliff^{*,a}, Nathan Harding^a, Mahendra Piraveenan^a, E. Yagmur Erten^{a,b},
Manoj Gambhir^c, Mikhail Prokopenko^{a,d}

^a Centre for Complex Systems, Faculty of Engineering and IT, University of Sydney, Sydney, NSW 2006, Australia

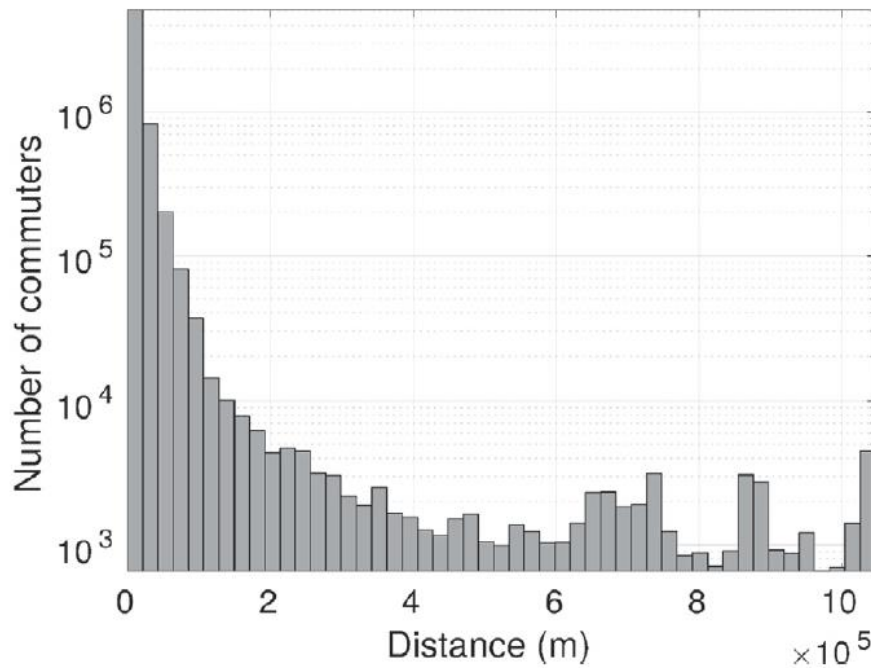
^b Department of Evolutionary Biology and Environmental Studies, University of Zurich, Winterthurerstrasse 190, Zurich, 8057, Switzerland

^c IBM Research, Melbourne, Australia

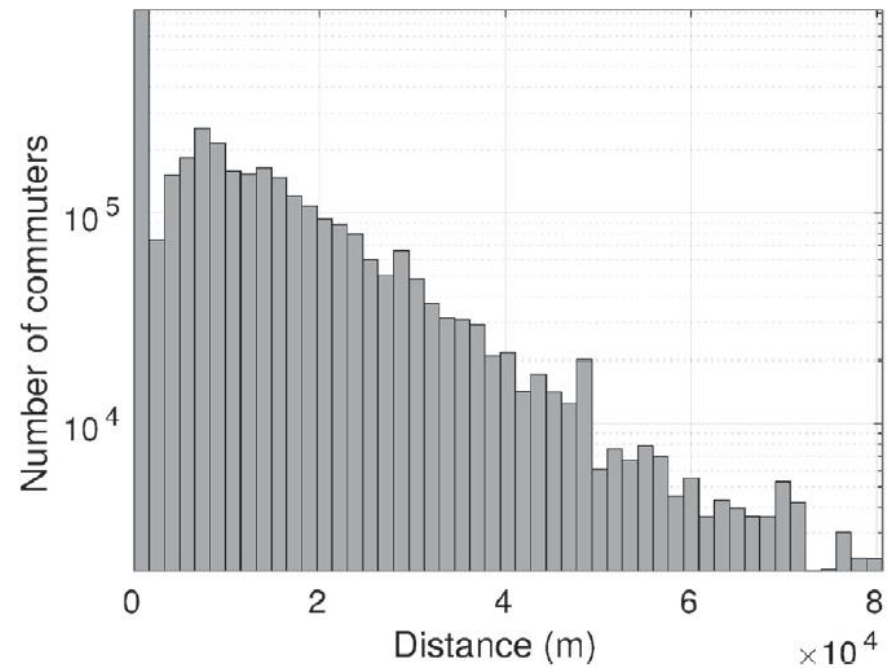
^d Marie Bashir Institute for Infectious Diseases and Biosecurity, University of Sydney, Westmead, NSW 2145, Australia



Australian Census: travel-to-work data (mobility)



(a) Workers



(b) Students

Fig. B1. Commute distance distributions.

Airport code	State	City	Passengers
SYD	NSW	Sydney	40884
MEL	VIC	Melbourne	25859
BNE	QLD	Brisbane	14250
PER	WA	Perth	11449
OOL	QLD	Gold Coast	3022
ADL	SA	Adelaide	2214
CNS	QLD	Cairns	1874
DRW	NT	Darwin	597
TSV	QLD	Townsville	105

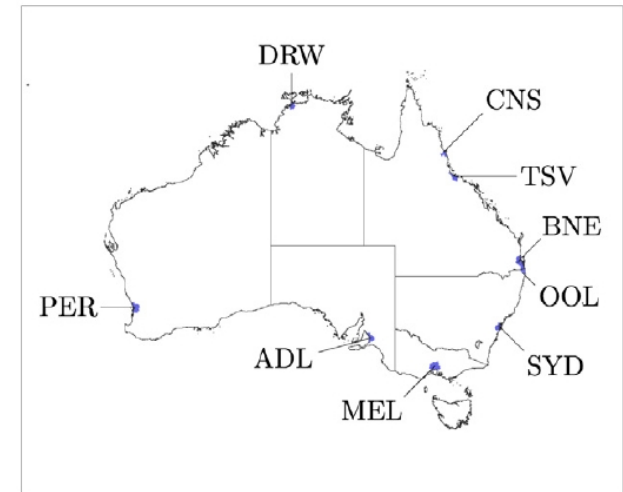
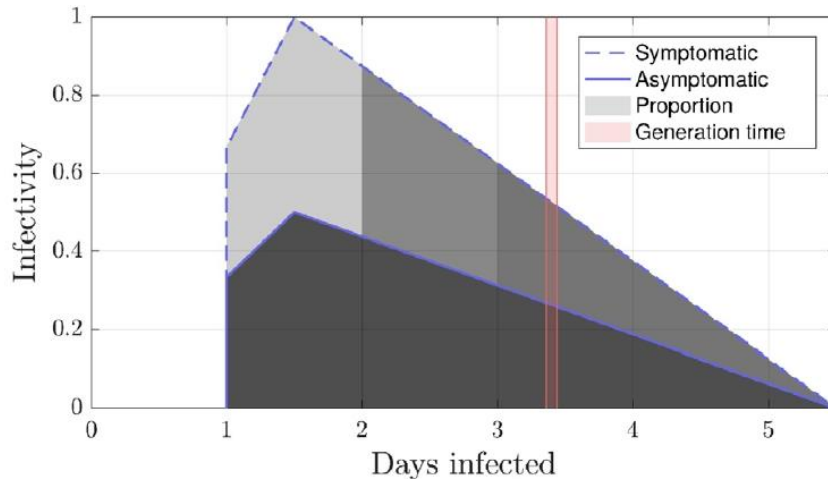
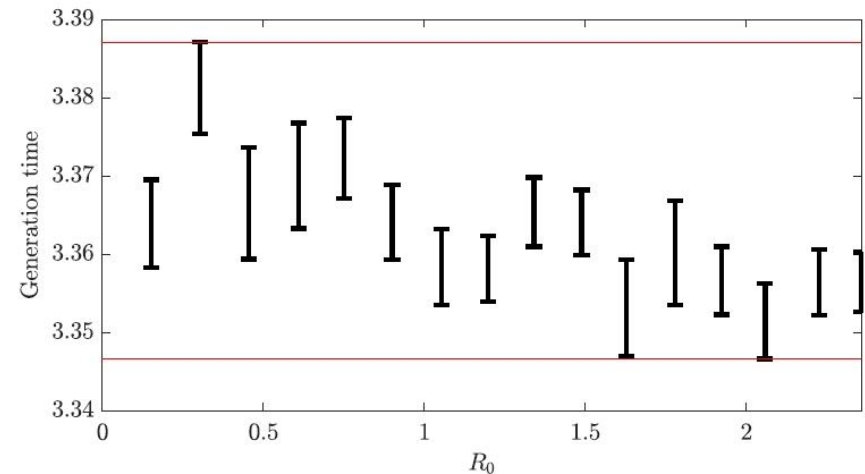


Fig. 3. Daily incoming passengers per Australian international airport obtained from BITRE [30] along with a map detailing the airport locations.

Epidemic modelling: natural history of the disease



(a) Natural history of the disease.

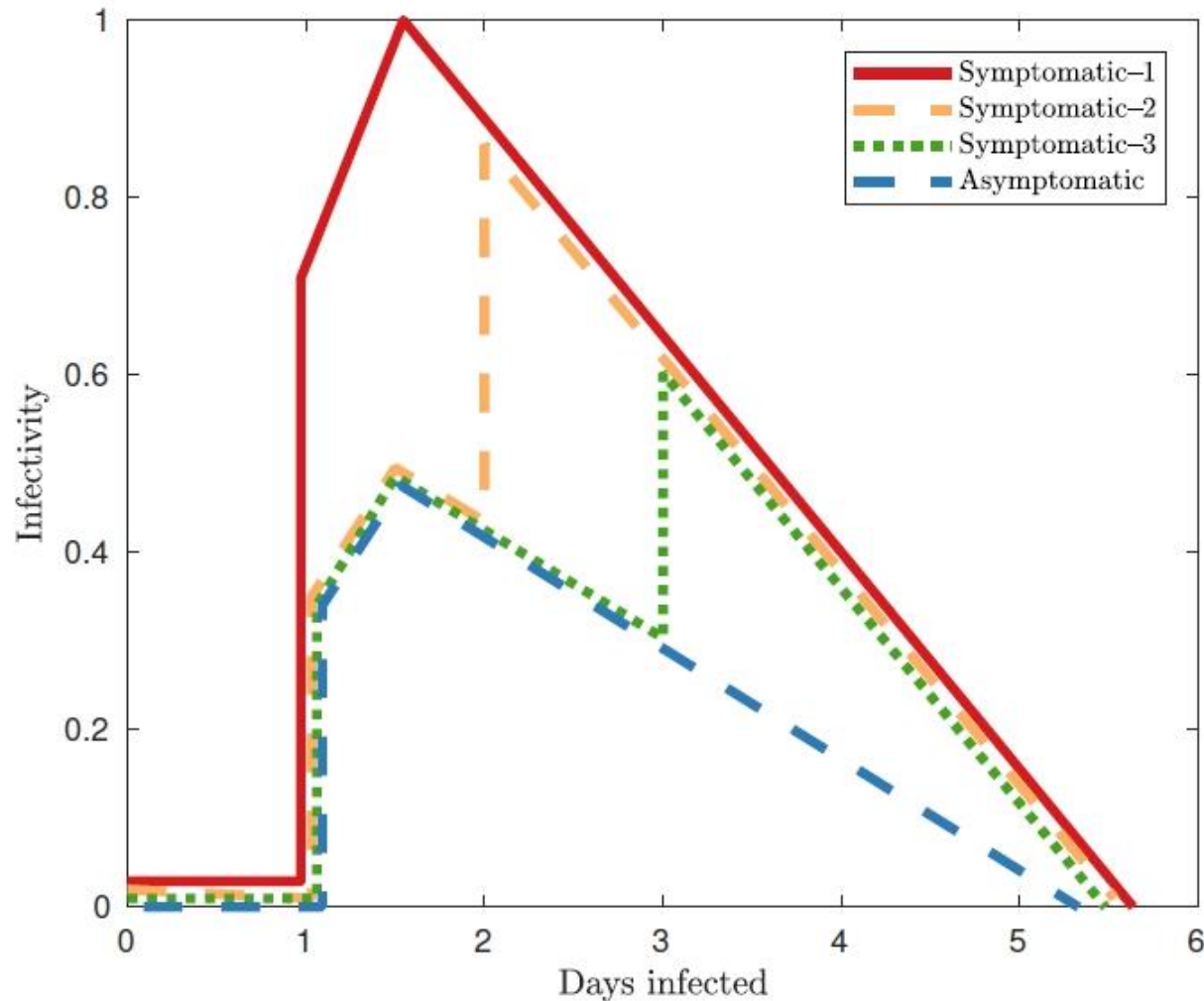


(b) Simulated generation time.

Fig. 2. Natural history of the disease and corresponding simulated generation time. The disease dynamics are modelled as having a linear increase followed by a linear decrease, as illustrated in Fig. 2 (a). In the figure, the area under the curve is shaded according to the proportion of people *at least* that infectious after disease onset (darker representing a higher proportion). If an agent becomes symptomatic, their infectiousness doubles (dashed blue line) from that day onward. Moreover, 67% of agents become symptomatic; of these agents, 30% start showing symptoms on day 1, 50% on day 2, and the remaining 20% on day 3. We obtain empirical generation times from simulations resulting from this model, shown in 2(b) for a number of R_0 values. The confidence intervals range from 3.35 to 3.39 days (also shown on Fig. 2(a)), depending on R_0 and, in general, the generation time has a slight downward trend as a function of disease severity.



Epidemic modelling: natural history of the disease



Epidemic modelling: transmission probabilities

Table C2

Daily transmission probabilities $q_{j \rightarrow i}^g$ for different contact groups g , obtained by Eq. (4) where $\beta_{j \rightarrow i}^g$ are reported by [10].

Contact Group g	Infected Individual j	Susceptible Individual i	Transmission Probability $q_{j \rightarrow i}^g$
Household size 2	Any	Child (< 19)	0.0933
	Any	Adult (> 18)	0.0393
Household size 3	Any	Child (< 19)	0.0586
	Any	Adult (> 18)	0.0244
Household size 4	Any	Child (< 19)	0.0417
	Any	Adult (> 18)	0.0173
Household size 5	Any	Child (< 19)	0.0321
	Any	Adult (> 18)	0.0133
Household size 6	Any	Child (< 19)	0.0259
	Any	Adult (> 18)	0.0107
School	Child (< 19)	Child (< 19)	0.000292
Grade	Child (< 19)	Child (< 19)	0.00158
Class	Child (< 19)	Child (< 19)	0.035

$$p_{j \rightarrow i}^g(n) = \kappa f(n - n_j \mid j) q_{j \rightarrow i}^g$$

$$p_i(n) = 1 - \prod_{g \in G_i(n)} \left[\prod_{j \in \mathcal{A}_g \setminus i} (1 - p_{j \rightarrow i}^g(n)) \right]$$

global scalar

$\beta / \gamma = R_0$

Role of social networks in shaping disease transmission during a community outbreak of 2009 H1N1 pandemic influenza

Simon Cauchemez^{a,1}, Achuyt Bhattarai^b, Tiffany L. Marchbanks^c, Ryan P. Fagan^b, Stephen Ostroff^c, Neil M. Ferguson^a, David Swerdlow^b, and the Pennsylvania H1N1 working group^{b,c,2}

^aMedical Research Council Centre for Outbreak Analysis and Modelling, Department of Infectious Disease Epidemiology, School of Public Health, Imperial College London, London W2 1PG, United Kingdom; ^bCenters for Disease Control and Prevention, Atlanta, GA 30333; and ^cPennsylvania Department of Health, Harrisburg, PA 17120-0701

Edited by David Cox, Nuffield College, Oxford, United Kingdom, and approved December 22, 2010 (received for review June 22, 2010)

Evaluating the impact of different social networks on the spread of respiratory diseases has been limited by a lack of detailed data on transmission outside the household setting as well as appropriate statistical methods. Here, from data collected during a H1N1 pandemic (pdm) influenza outbreak that started in an elementary school and spread in a semirural community in Pennsylvania, we quantify how transmission of influenza is affected by social networks. We set up a transmission model for which parameters are estimated from the data via Markov chain Monte Carlo sampling. Sitting next to a case or being the playmate of a case did not significantly increase the risk of infection; but the structuring of

sylvania to investigate how social networks and population structures affect influenza transmission.

Results and Discussion

Outbreak Investigation. Fig. 1 presents the data that were collected during the outbreak investigation. Demographic and clinical information on 370 (81%) students from 295 (81%) households and their 899 household contacts was collected during two rounds of phone interviews (May 16–21 and May 26–June 2). One hundred twenty-nine (35%) students and 141 (16%) household contacts were reported to have had acute re-



Social interactions (Cauchemez et al., 2010)

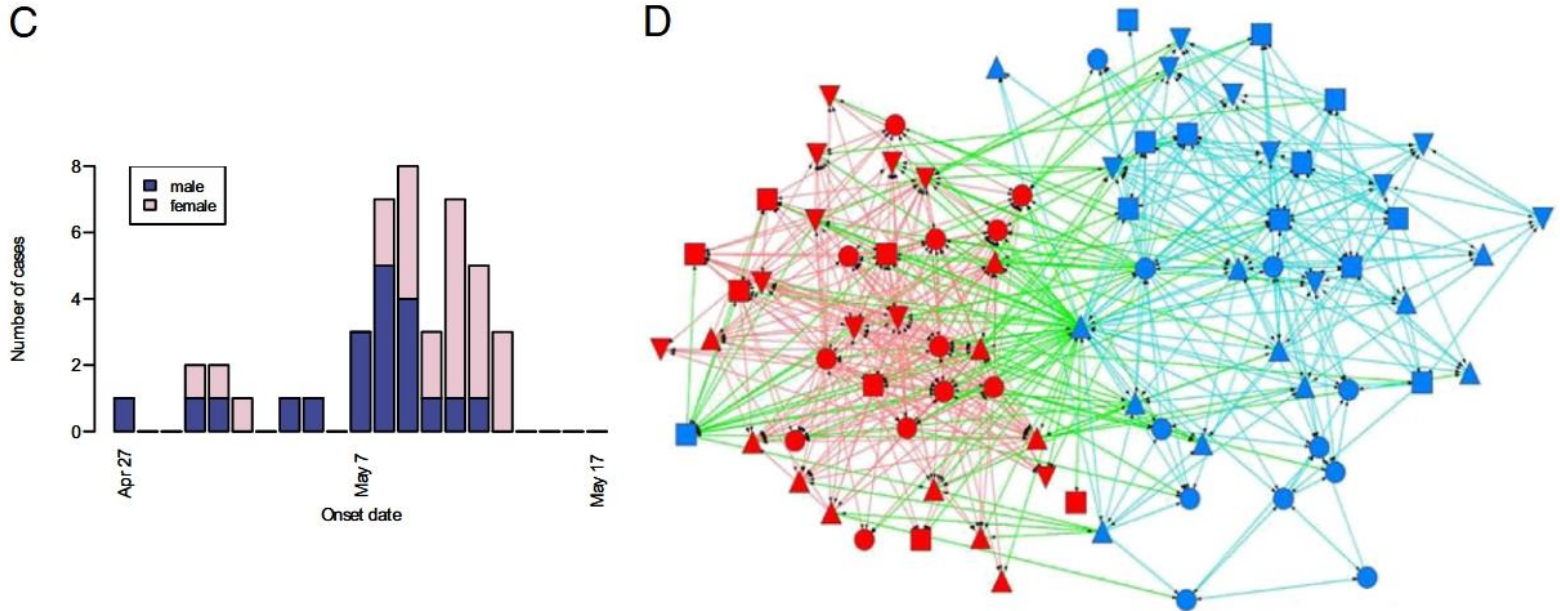


Fig. 1. Epidemiological data collected in the school. (A) Number of acute respiratory illness (ARI) cases by date of symptom onset for different types of individuals. (B–D) Survey of fourth graders with (B) seating charts and diagnosis for ARI in classroom C, (C) number of ARI cases by date of symptom onset and sex among fourth graders, and (D) social networking among fourth graders based on the question “Who are your playmates?” [color of the nodes, red, female; blue, male; color of the lines, red, girl–girl interaction; cyan, boy–boy interaction; green, boy–girl interaction (one symbol shape per class)]. The algorithm used to draw the network aims at (i) distributing nodes evenly, (ii) making edge length uniform, (iii) minimizing edge crossings, and (iv) keeping nodes from coming too close to edges (32, 33) (software: *Netdraw*). It does not use data on sex to position the nodes.

Table C1

Daily contact probabilities $c_{j \rightarrow i}^g$ for different contact groups g , reported by [22].

Mixing group g	Infected individual j	Susceptible individual i	Contact probability $c_{j \rightarrow i}^g$
Household cluster	Child (<19)	Child (<19)	0.08
	Child (<19)	Adult (>18)	0.035
	Adult (>18)	Child (<19)	0.025
	Adult (>18)	Adult	0.04
Working Group	Adult (19-64)	Adult (19-64)	0.05
Neighbourhood	Any	Child (0-4)	0.0000435
	Any	Child (5-18)	0.0001305
	Any	Adult (19-64)	0.000348
	Any	Adult (65+)	0.000696
Community	Any	Child (0-4)	0.0000109
	Any	Child (5-18)	0.0000326
	Any	Adult (19-64)	0.000087
	Any	Adult (65+)	0.000174

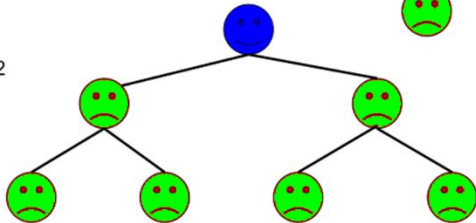


Epidemic modelling: reproductive ratio R_0

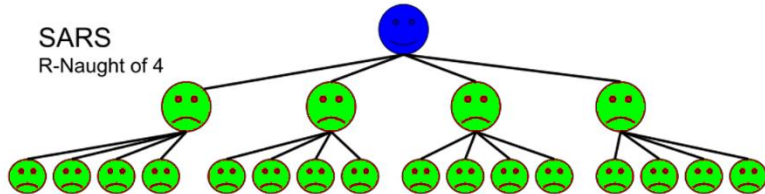
● Patient Zero

● Infected

Ebola:
R-Naught of 2



SARS
R-Naught of 4



$$\frac{dS}{dt} = \gamma I - \beta IS$$

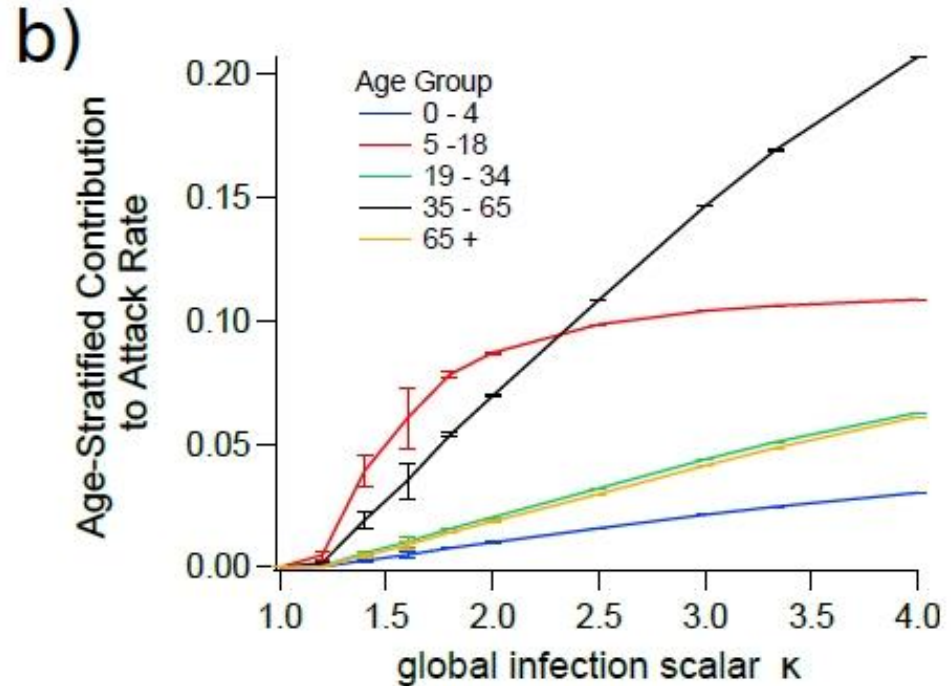
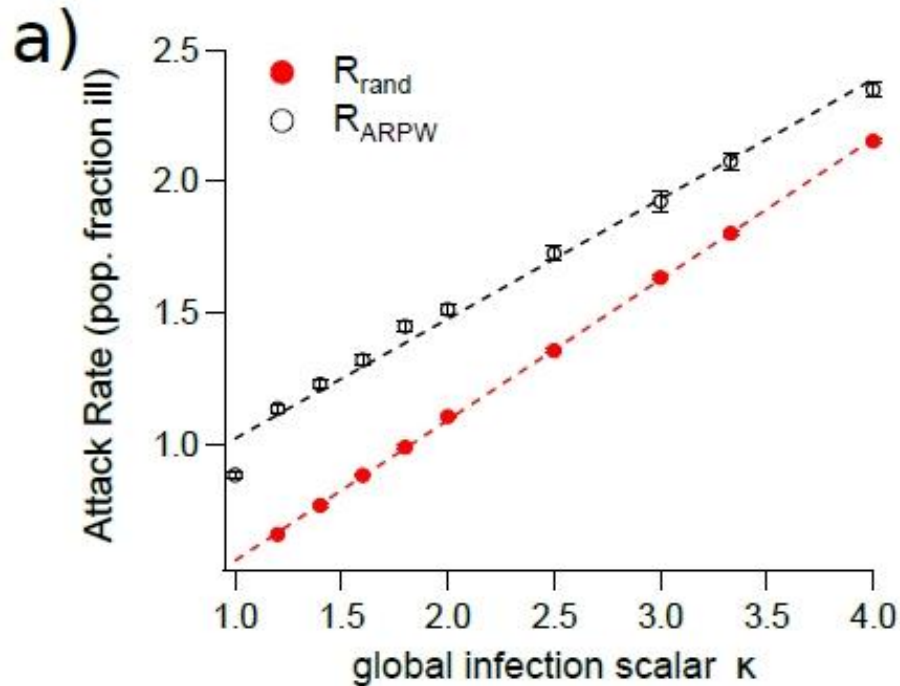
$$\frac{dI}{dt} = \beta IS - \gamma I$$

$$\beta / \gamma = R_0$$

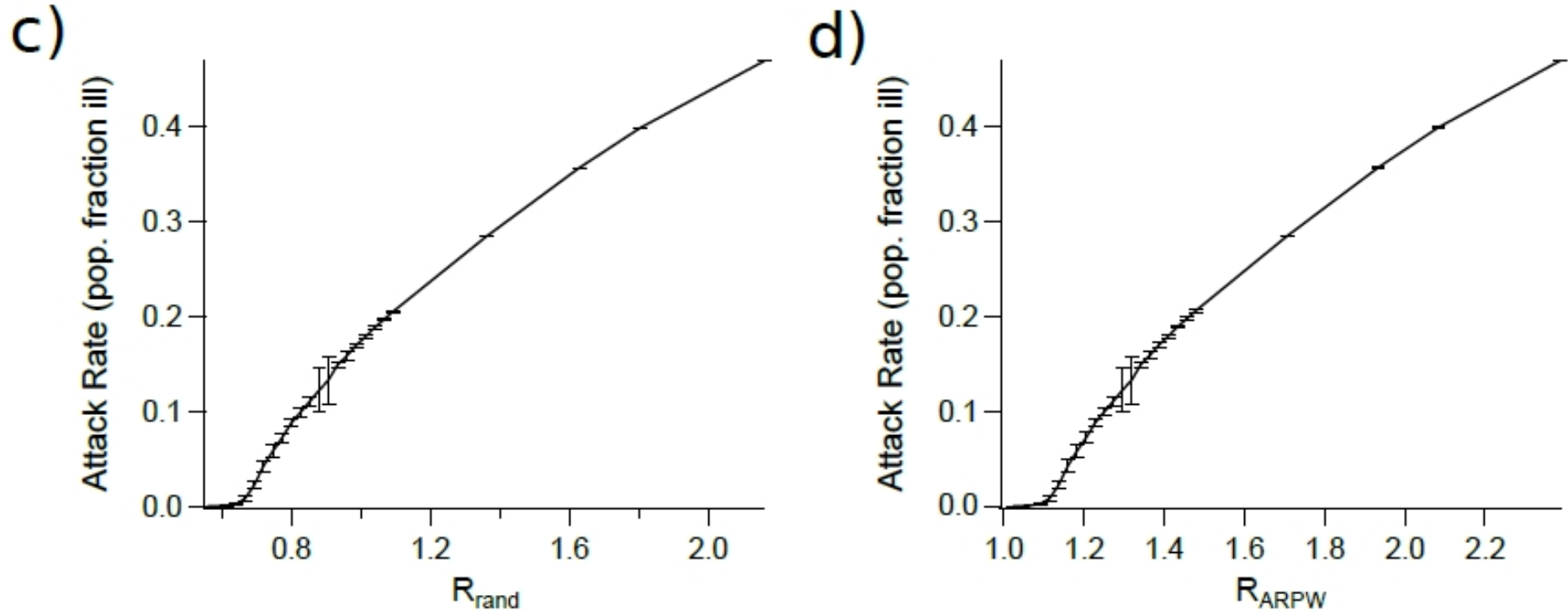
$$\begin{aligned}
 R_0 &= \mathbb{E} \left(\sum_i X_i(N) = \text{SYMPTOMATIC} \mid X_J(0) = \text{SYMPTOMATIC} \right) \\
 &= \mathbb{E} \left(\mathbb{E} \left(\prod_n p_I(n) \mid X_J(0) = \text{SYMPTOMATIC} \right) \right) \\
 &= \sum_j \sum_i \prod_n \left(1 - \prod_{g \in \mathcal{G}_j(n)} \left(1 - p_{j \rightarrow i}^g(n) \right) \right),
 \end{aligned}$$



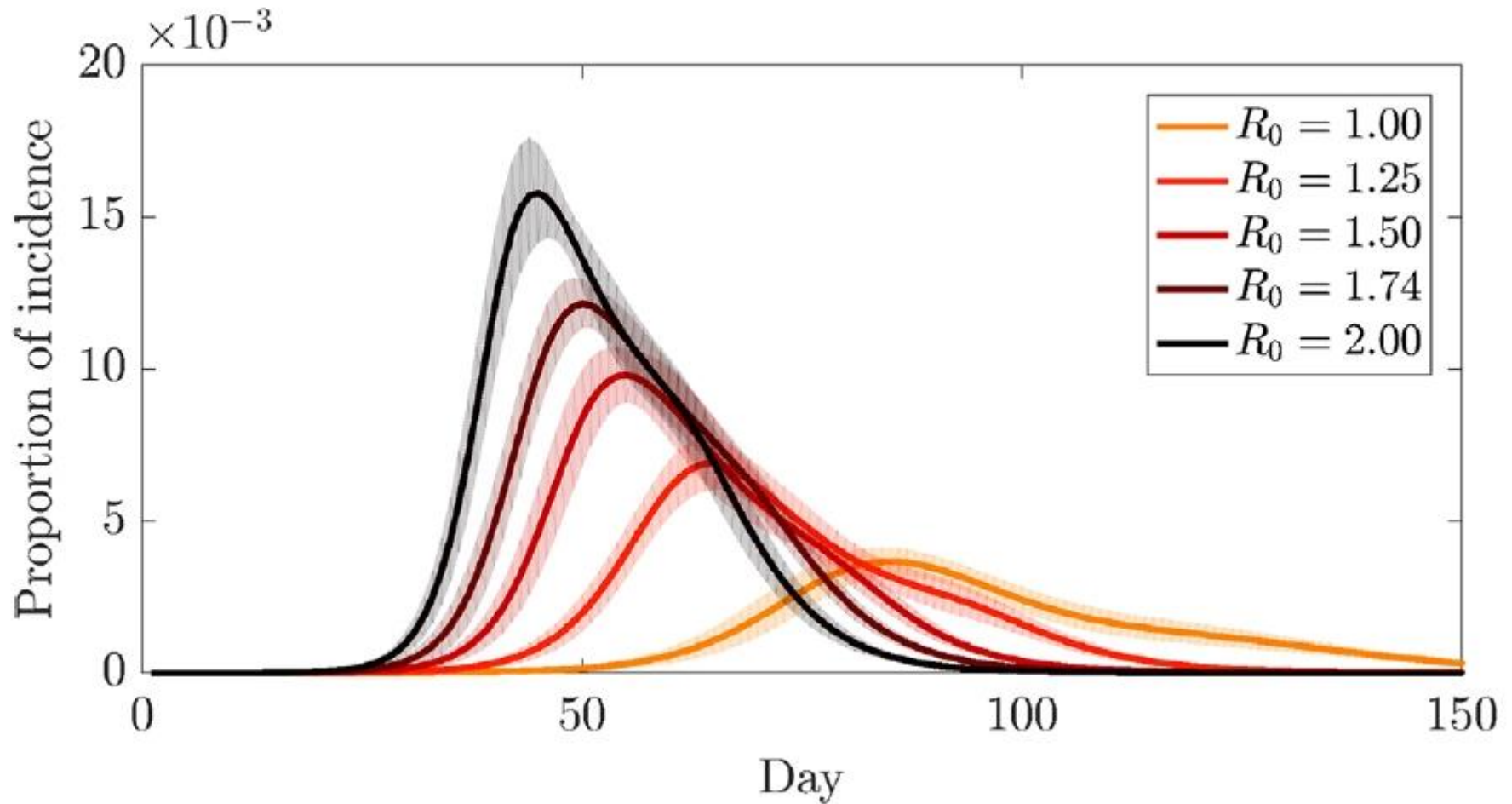
Epidemic modelling: reproductive ratio R_0



Epidemic modelling: reproductive ratio R_0

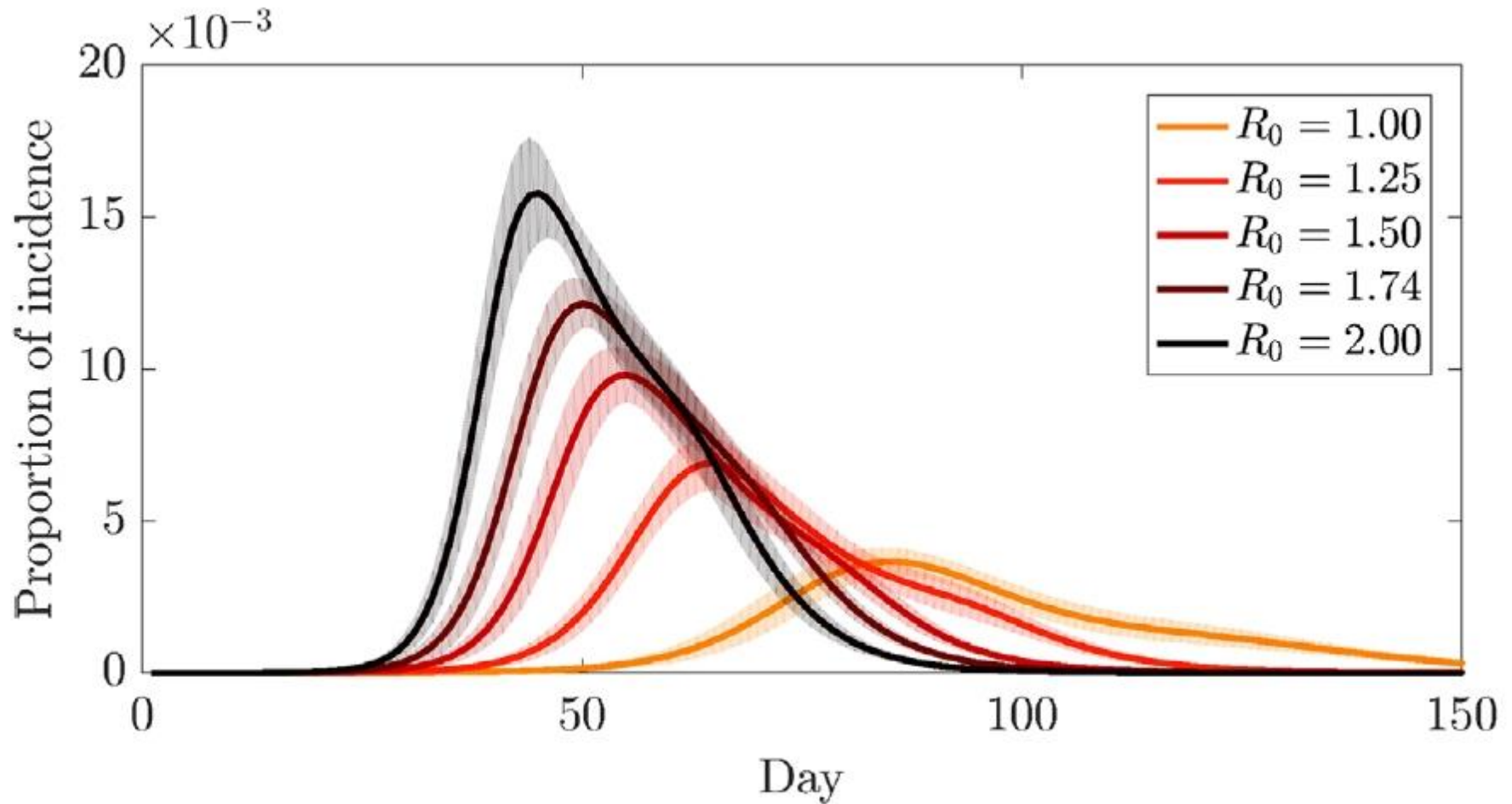


Epidemic modelling: reproductive ratio R_0





Epidemic modelling: reproductive ratio R_0



“herd immunity” threshold: $1 - 1/R_0$

Hierarchical spatial spread or wave-like diffusion??

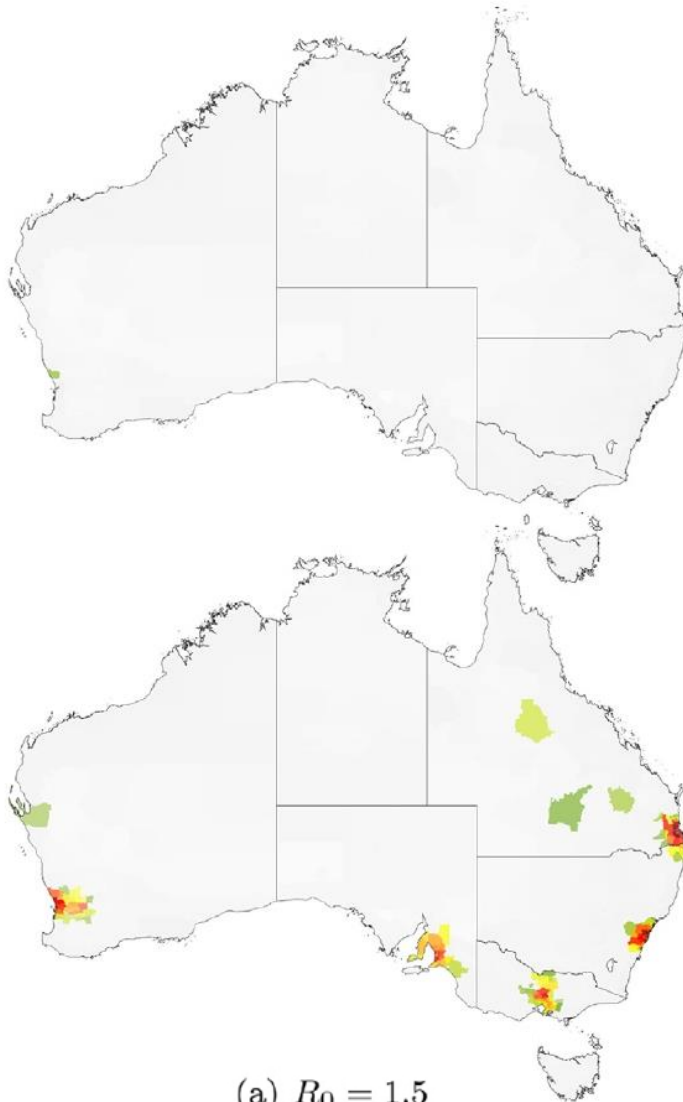
C. Viboud, O.N. Bjørnstad, D.L. Smith, L. Simonsen, M.A. Miller, B.T. Grenfell, Synchrony, waves, and spatial hierarchies in the spread of influenza, *Science* 312 (5772) (2006) 447–451.

The regional spread of infection correlates more closely with rates of movement of people to and from their workplaces (workflows) than with geographical distance.

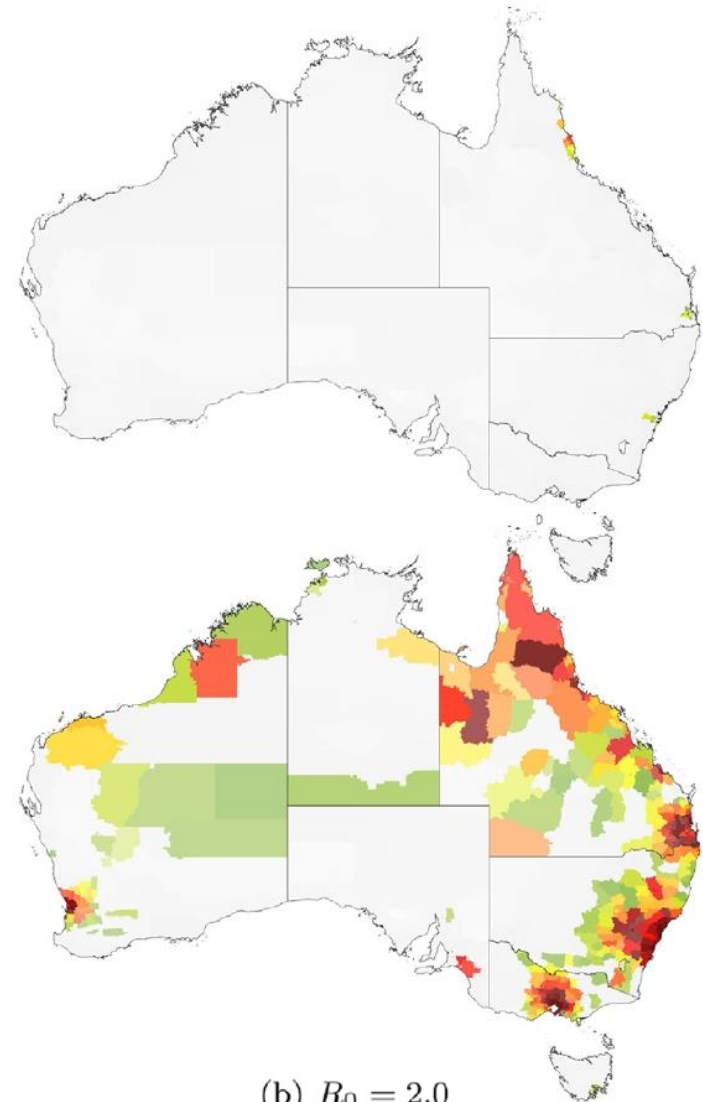
The hierarchy of spread is immediately apparent: The most populous states exhibit synchronized epidemics, whereas less populated states exhibit more erratic patterns, both relative to each other and to the continental norm.



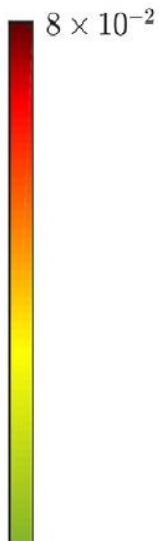
Time



(a) $R_0 = 1.5$



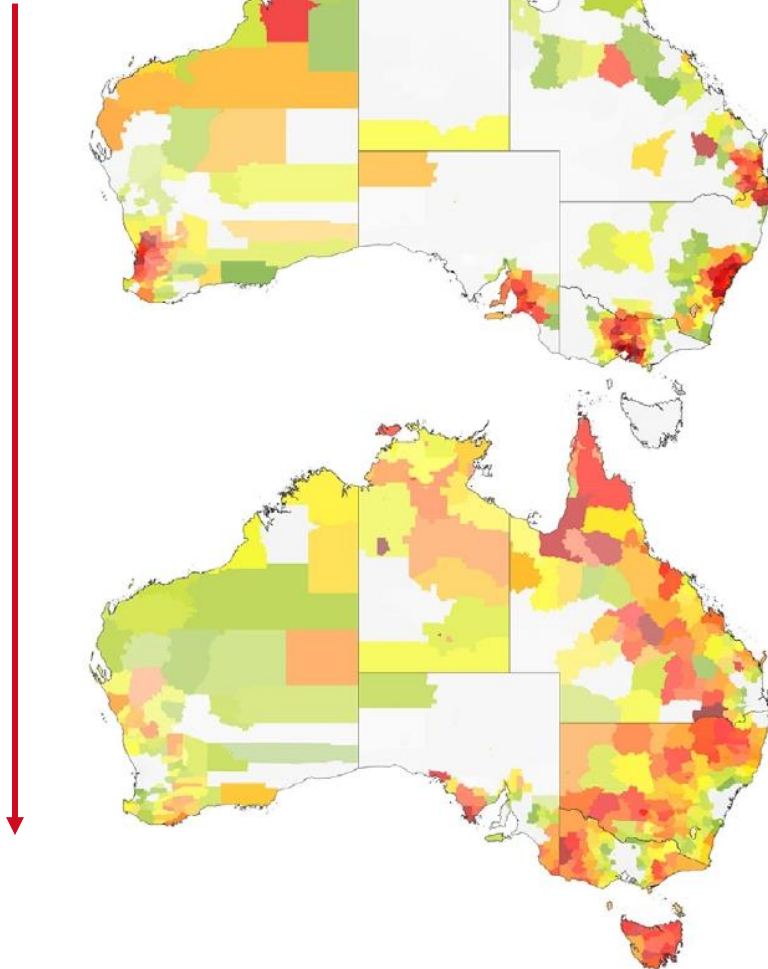
(b) $R_0 = 2.0$



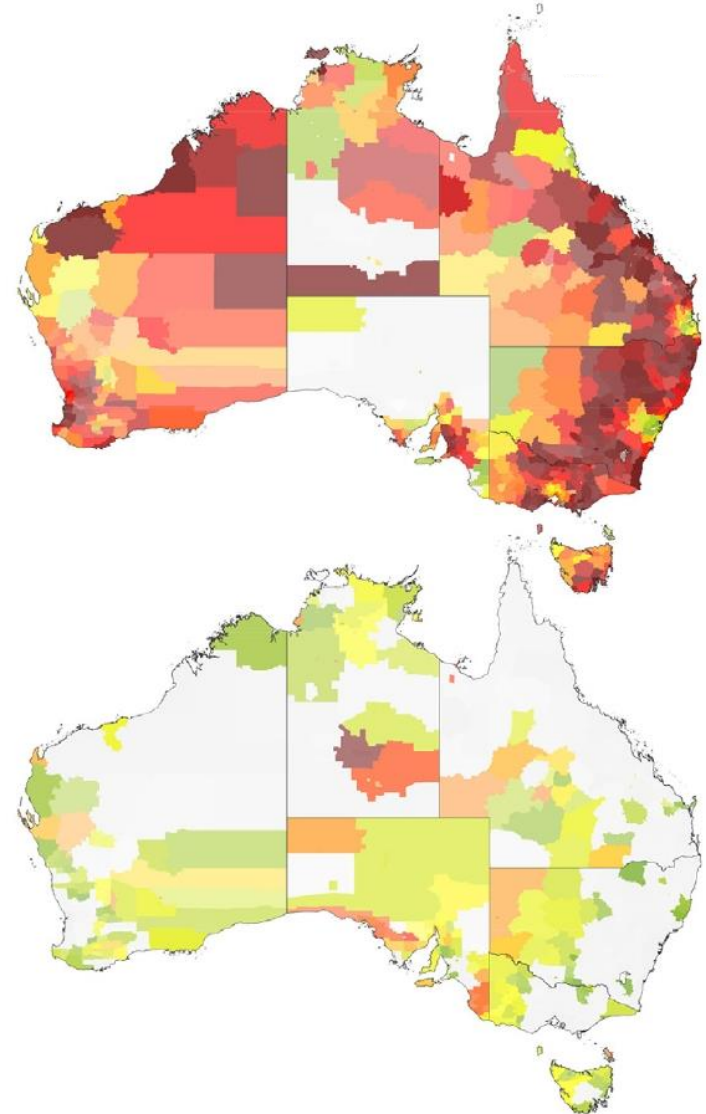


Spatiotemporal synchrony

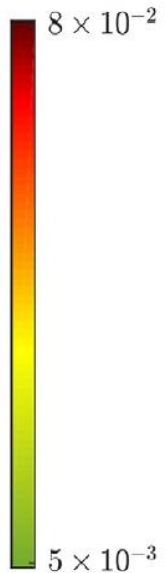
Time



(a) $R_0 = 1.5$

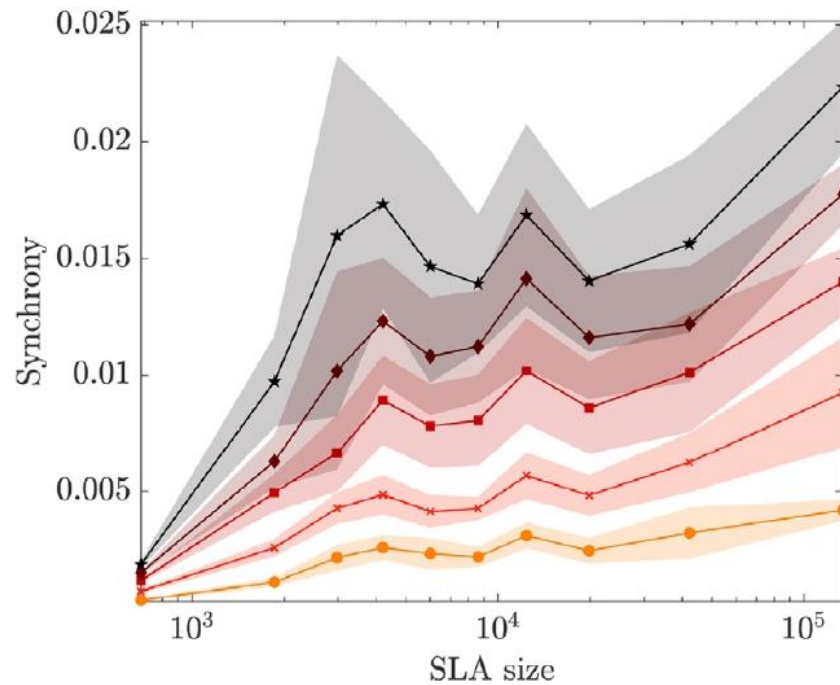


(b) $R_0 = 2.0$

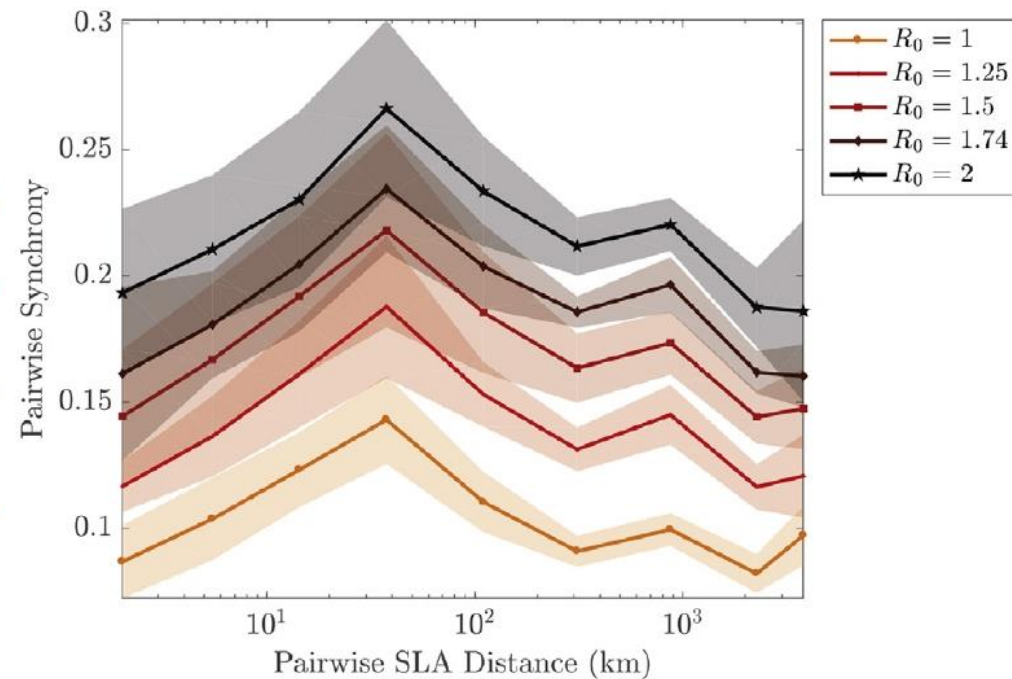




Hierarchical spatial spread or wave-like diffusion??



(a)



(b)

RESEARCH ARTICLE | SOCIAL SCIENCES

Urbanization affects peak timing, prevalence, and bimodality of influenza pandemics in Australia: Results of a census-calibrated model

Cameron Zachreson^{1,*}, Kristopher M. Fair¹, Oliver M. Cliff¹, Nathan Harding¹, Mahendra Piraveenan¹ and Mikhail Prokopenko^{1,2}

¹Complex Systems Research Group, School of Civil Engineering, Faculty of Engineering and IT, The University of Sydney, Sydney, NSW 2006, Australia.

²Marie Bashir Institute for Infectious Diseases and Biosecurity, The University of Sydney, Westmead, NSW 2145, Australia.

✉*Corresponding author. Email: cameron.zachreson@sydney.edu.au

– Hide authors and affiliations

Science Advances 12 Dec 2018:
Vol. 4, no. 12, eaau5294
DOI: 10.1126/sciadv.aau5294

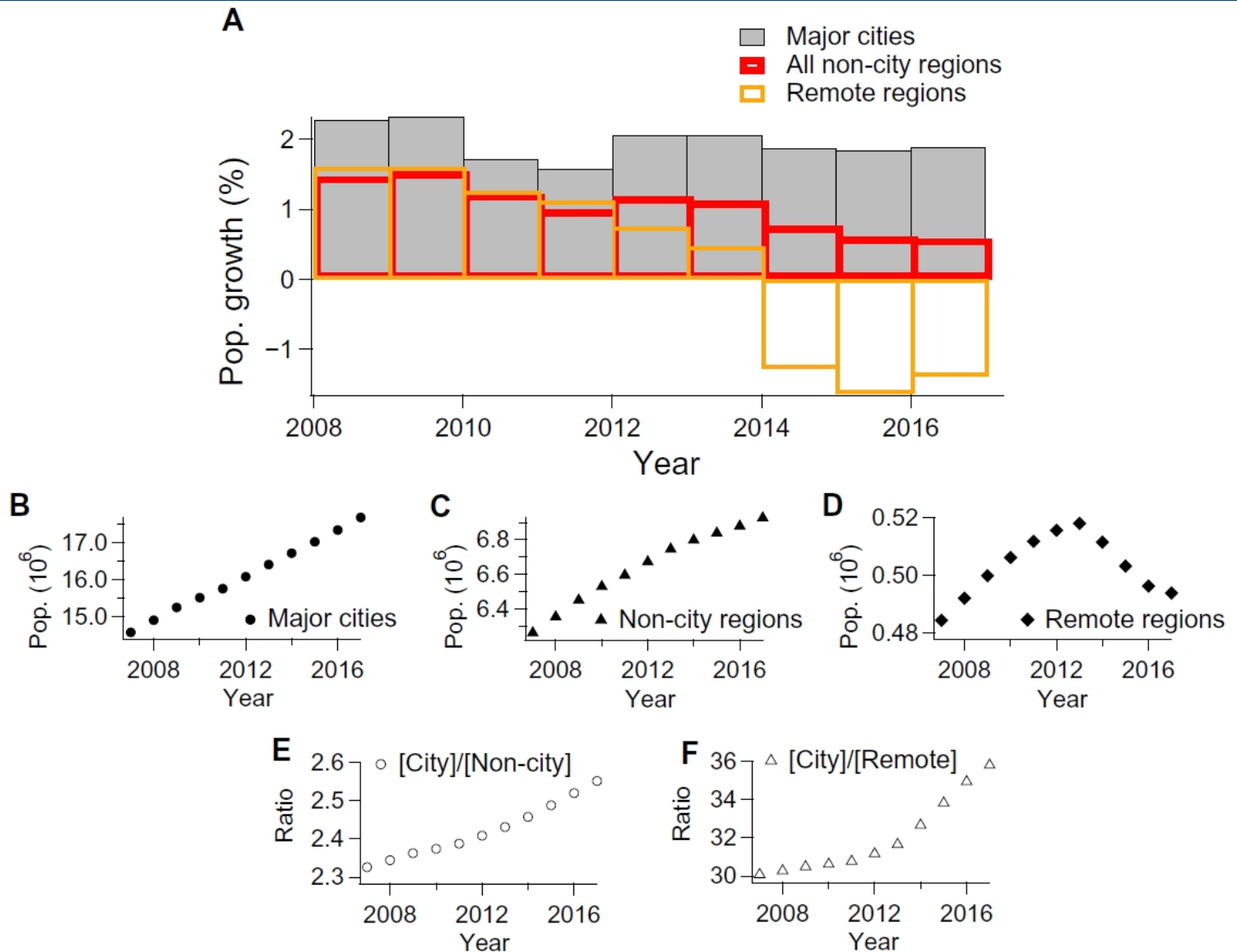


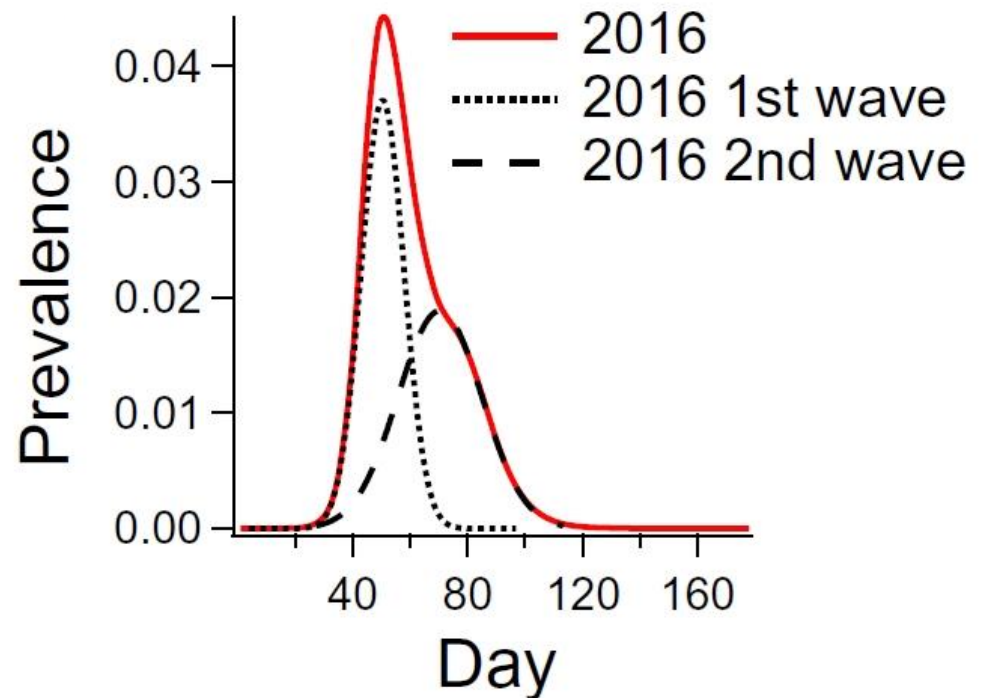
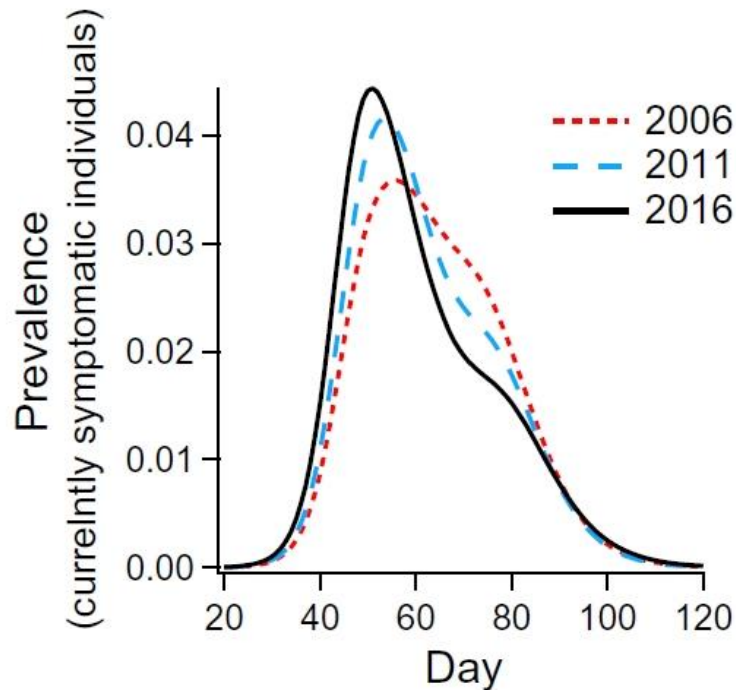


Table 1. Average daily incoming international air traffic.

Airport	State	Year		
		2006	2011	2016
Sydney	New South Wales	13,214	15,995	19,991
Melbourne	Victoria	5,923	8,557	12,802
Brisbane	Queensland	5,053	5,946	7,299
Perth	Western Australia	2,766	4,512	5,906
Gold Coast	Queensland	285	1,044	1,435
Adelaide	South Australia	492	766	1,170
Cairns	Queensland	1,186	707	824
Darwin	Northern Territory	160	356	355
Townsville	Queensland	0	11	39

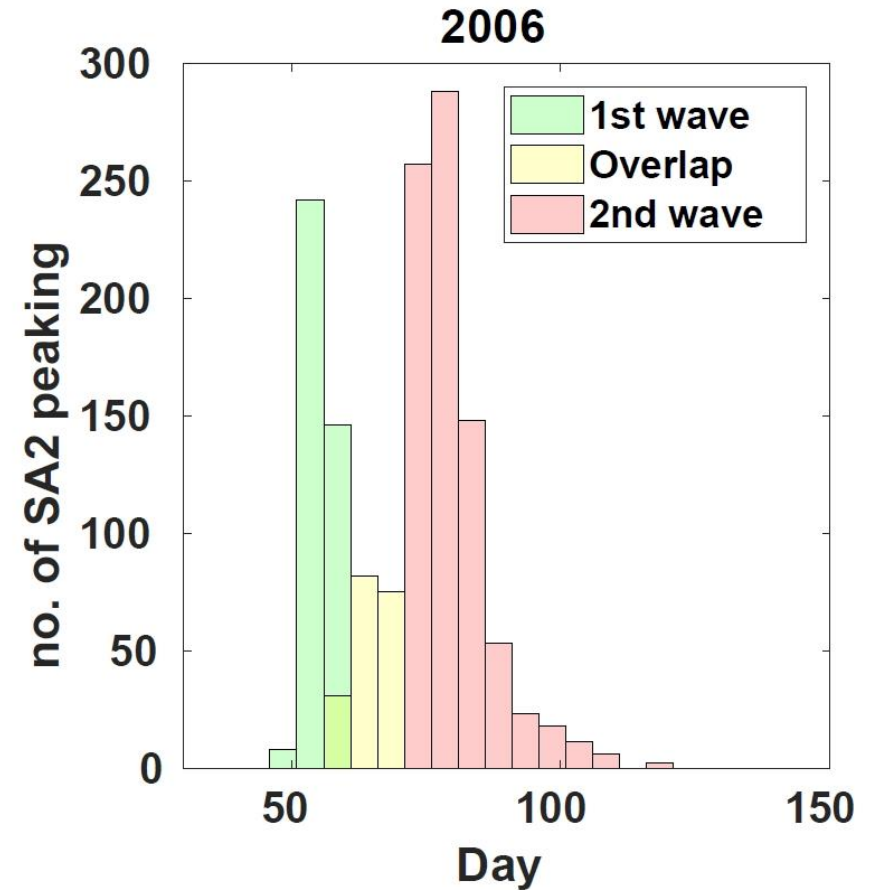
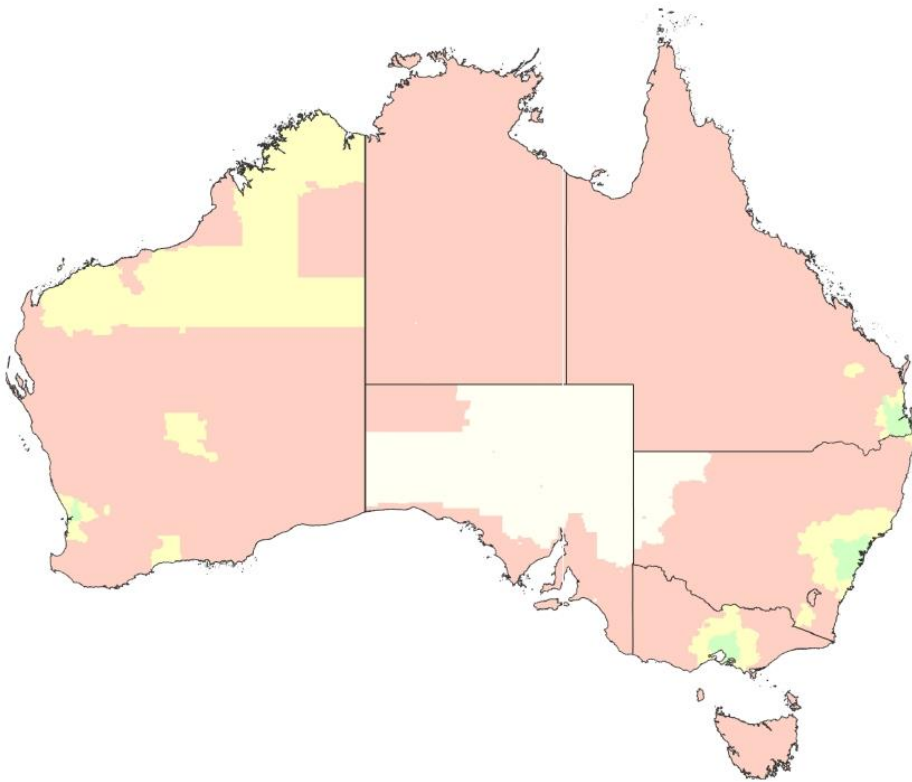


Prevalence and epidemic peaks: H1N1



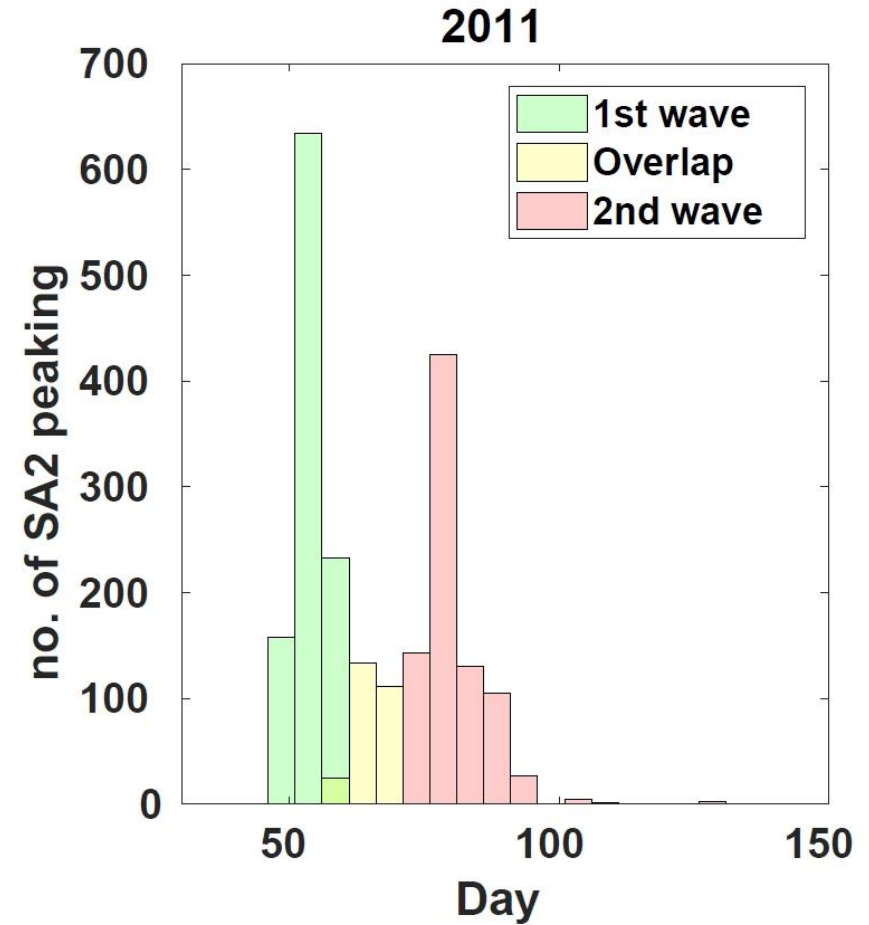
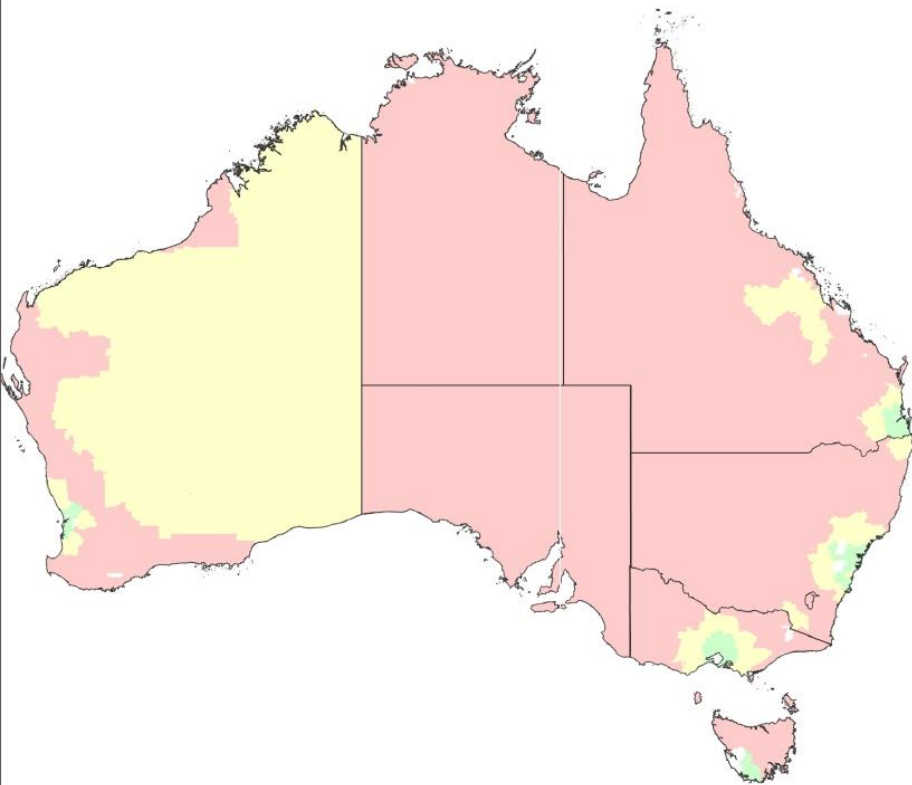


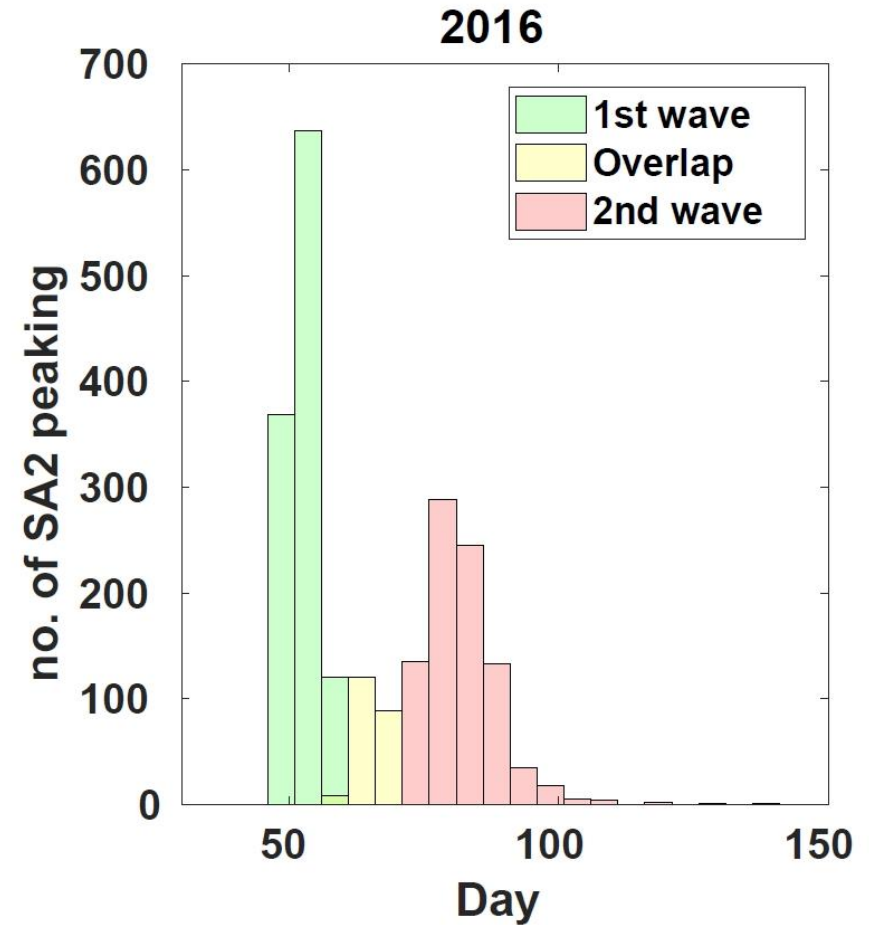
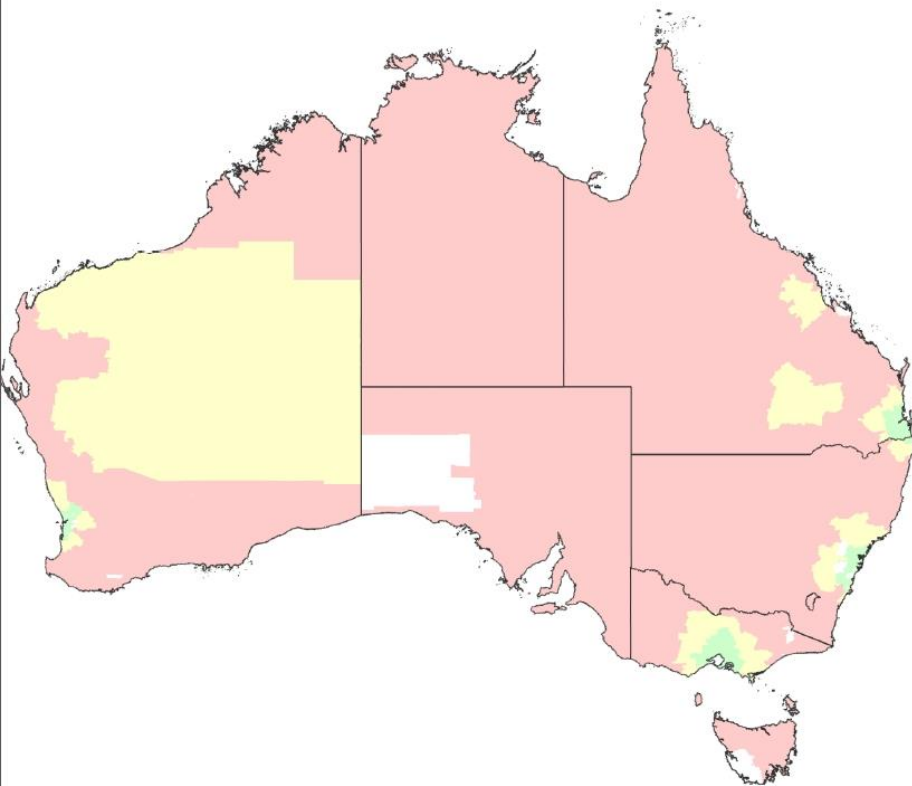
Bimodality: 2006





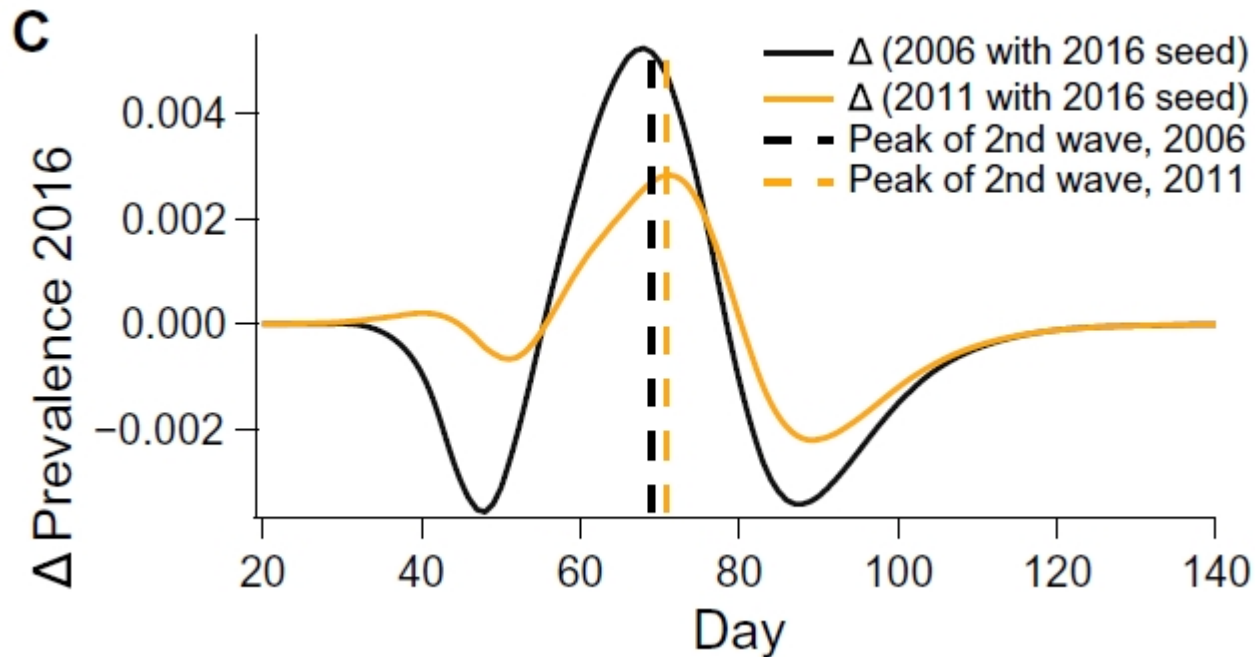
Bimodality: 2011







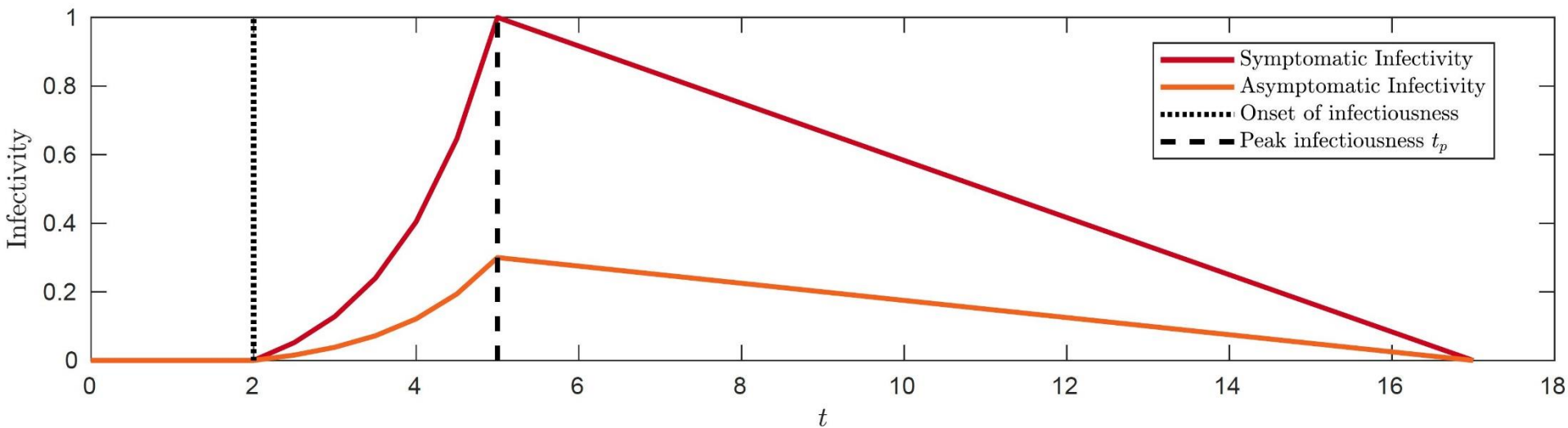
Key factors: higher urbanisation or more air traffic?



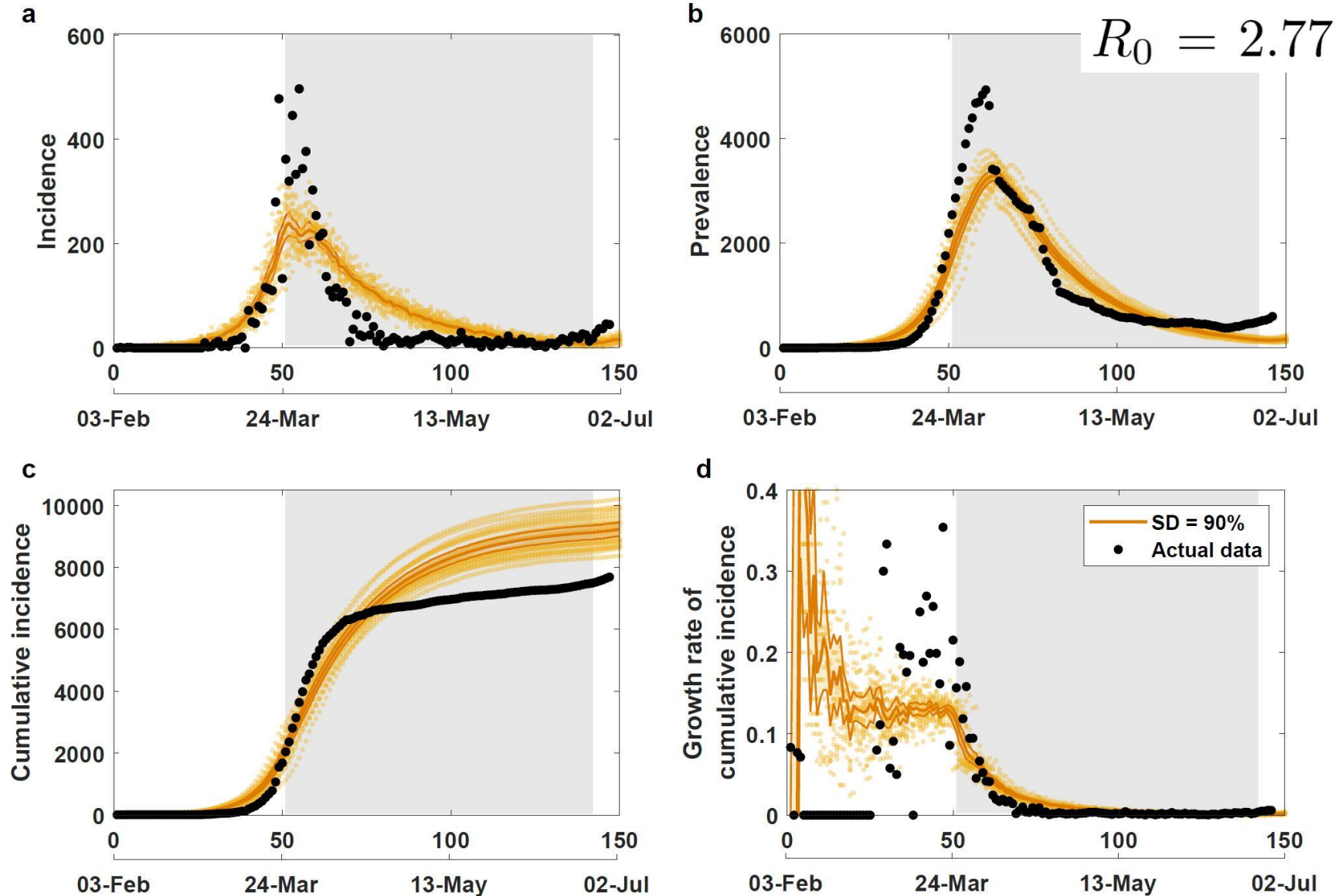
- seeding conditions have a larger impact on the first wave than on the second
- seeding does not account for the decrease in the intensity of the second pandemic wave from year to year, a trend that we ascribe to increased urbanisation



COVID-19: natural history of the disease (our 2020 model: AMTraC-19 version 6.1)



AMTraC-19 validation (version 6.1)





Social Distancing (SD): “stay-at-home” restrictions

Table 2 The micro- and macro-distancing parameters: macro-compliance levels and context-dependent micro-distancing levels.

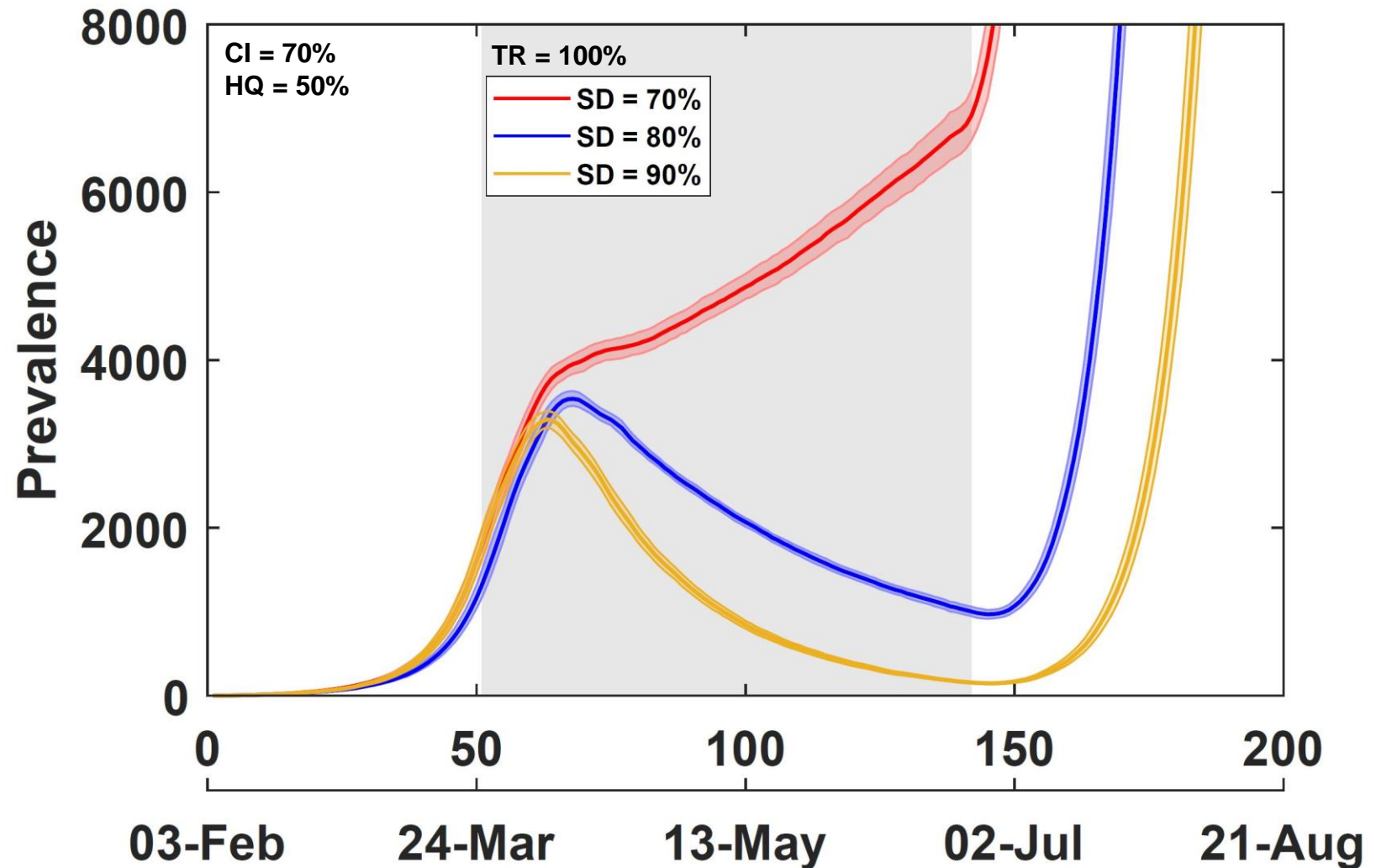
Strategy	Macro-distancing	Micro-distancing contacts		
	Compliance levels	Household	Community	Workplace/school
No intervention	100%	100%	100%	100%
Case isolation	70%	100%	25%	25%
Home quarantine	50%	200%	25%	25%
School closure (children)	100%	150%	150%	0%
School closure (parents)	25 or 50%	150%	150%	0%
Social distancing	0-100%	100%	50%	0%

$$p_i(n) = 1 - \prod_{g \in G_i(n)} \left[\prod_{j \in A_g \setminus i} (1 - p_{j \rightarrow i}^g(n)) \right]$$

$$p_i(n) = 1 - \prod_{g \in G_i(n)} \left[1 - F_g(i) \left(1 - \prod_{j \in A_g \setminus \{i\}} (1 - F_g(j) p_{j \rightarrow i}^g(n)) \right) \right]$$



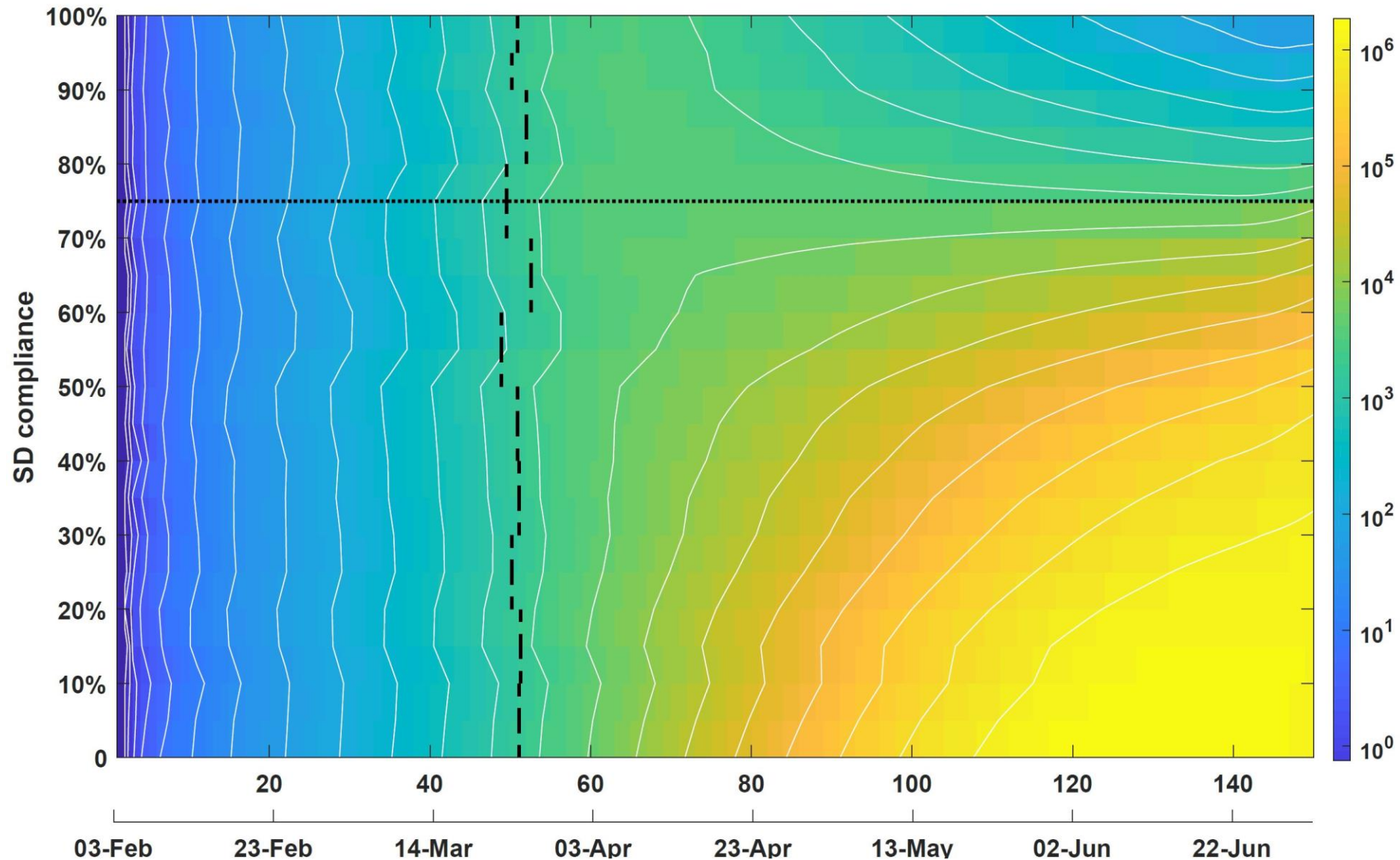
2020 model: a tipping point in social distancing





THE UNIVERSITY OF
SYDNEY

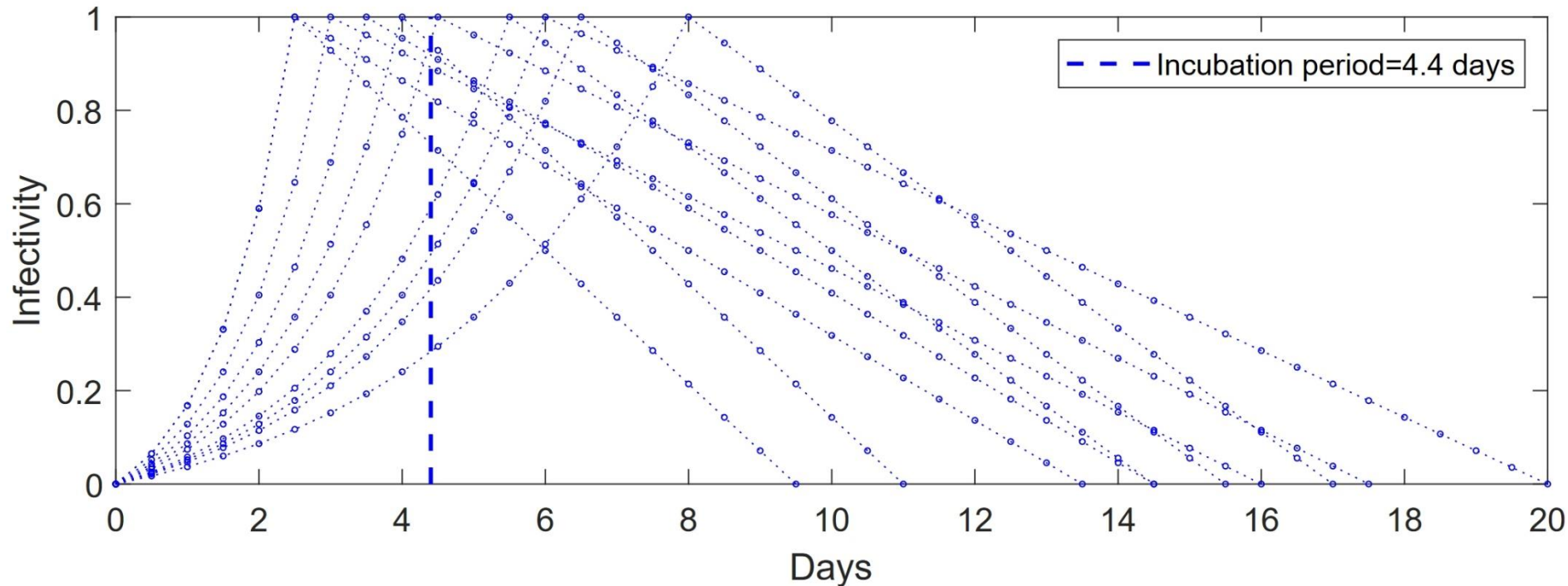
Tipping point (phase transition) in SD compliance



Natural history of the disease (our 2021 model: AMTraC-19 version 7.6)

- infectious incubation period is log-normally distributed with mean ~~5.5~~ 4.4 days
- infectious asymptomatic or symptomatic period, following incubation, lasts between 7 and 14 days (uniformly distributed with mean 10.5 days)
- differentiation between:
 - “asymptomatic infectivity” (factor of 0.5) and
 - “pre-symptomatic infectivity” (factor of 1.0)
- detection probabilities:
 - symptomatic (detection per day is 0.23)
 - pre-symptomatic and asymptomatic (detection per day is 0.01)

Natural history of the disease (the Delta variant model: AMTraC-19 version 7.7)



	R_0	T_{gen} (days)	T_{inc} (days)	T_{rec} (days)
Mean	6.2	6.93	4.4	10
95% CI	6.16 – 6.23	6.87 – 6.99	3.9 – 5.0	range: 7 – 14 (uniform)

Parameters (the Delta variant model: AMTraC-19 version 7.7)

Table S3. Main parameters for AMTraC-19 transmission model.



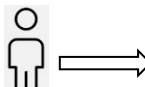
parameter	value	distribution	notes
κ	5.3	NA	global transmission scalar
T_{inc}	4.4 days (mean)	lognormal ($\mu = 1.396, \sigma = 0.413$)	incubation period
T_{rec}	10.5 days (mean)	uniform [7, 14] days	symptomatic (or asymptomatic) period
α	0.5	NA	asymptomatic transmission scalar
ρ	0.08	NA	contact-to-transmission scalar
σ_a	0.67	NA	probability of symptoms in adults (age > 18)
σ_c	0.134 or 0.268	NA	probability of symptoms in children (age ≤ 18)
r_{symp}	0.227	NA	daily case detection rate (symptomatic)
r_{asymp}	0.01	NA	daily case detection rate (asymptomatic)



Social distancing (SD): “stay-at-home” restrictions

NPI	Compliance	Interaction strength		
		Household	Community	Workplace
Case isolation	0.7 – 0.8	1.0	0.1 – 0.25	0.1 – 0.25
Home quarantine	0.5 – 0.7	2.0	0.1 – 0.25	0.1 – 0.25
School (students)	1.0	1.0	0.1 – 0.5	0.0
School (parents)	0.5	1.0	0.1 – 0.5	0.0
Social distancing	0.0 – 1.0	1.0	0.1 – 0.25	0.1

Modelling vaccination rollout (our 2021 model: AMTraC-19 version 7.6)

- Efficacy for susceptibility (**VEs**): impacts immunity in those susceptible to the virus (reduces the probability of becoming infected if exposed) 
- Efficacy for disease (**VEd**): impacts the expression of illness in those who are vaccinated and subsequently become infected (reduces the probability of expressing symptoms if infected) 
- Efficacy for infectiousness (**VEi**): impacts the potential for vaccinated individuals to transmit the virus if infected (reduces the force of infection produced by infected individuals who are vaccinated) 

$$VE = VEd + VEs - VEs \times VEd$$

$$VEi = \sim 0.5$$

for example:

$$0.91 = 0.7 + 0.7 - 0.7 \times 0.7$$

$$0.92 = 0.8 + 0.6 - 0.8 \times 0.6$$

$$0.75 = 0.5 + 0.5 - 0.5 \times 0.5$$

$$0.65 = 0.5 + 0.3 - 0.5 \times 0.3$$

Vaccine efficacy and herd immunity (...textbook)

Vaccine efficacy: $VE = 1 - \text{risk}$

where **risk** is relative risk for developing a **condition** in vaccinated people compared to unvaccinated people

Herd immunity threshold:

$$\frac{1 - 1/R_0}{VE}$$

$R_0 = 2.75$ and $VE = 0.9$:

$$\frac{1 - 1/2.75}{0.9} = 0.707$$

$R_0 = 5.5$ and $VE = 0.8$:

$$\frac{1 - 1/5.5}{0.8} = 1.023$$



Vaccination components

$$p_i(n) = 1 - \prod_{g \in G_i(n)} \left[\prod_{j \in A_g \setminus i} (1 - p_{j \rightarrow i}^g(n)) \right]$$

$$p_i(n) = 1 - \prod_{g \in G_i(n)} \left[1 - F_g(i) \left(1 - \prod_{j \in A_g \setminus \{i\}} (1 - F_g(j) p_{j \rightarrow i}^g(n)) \right) \right]$$

$$p_i(n) = 1 - \prod_{g \in G_i(n)} \left[1 - \overset{\implies \text{person}}{(1 - V E_i^s) F_g(i)} \left(1 - \prod_{j \in A_g \setminus i} \overset{\text{person} \implies}{(1 - (1 - V E_j^t) F_g(j) p_{j \rightarrow i}^g(n))} \right) \right]$$

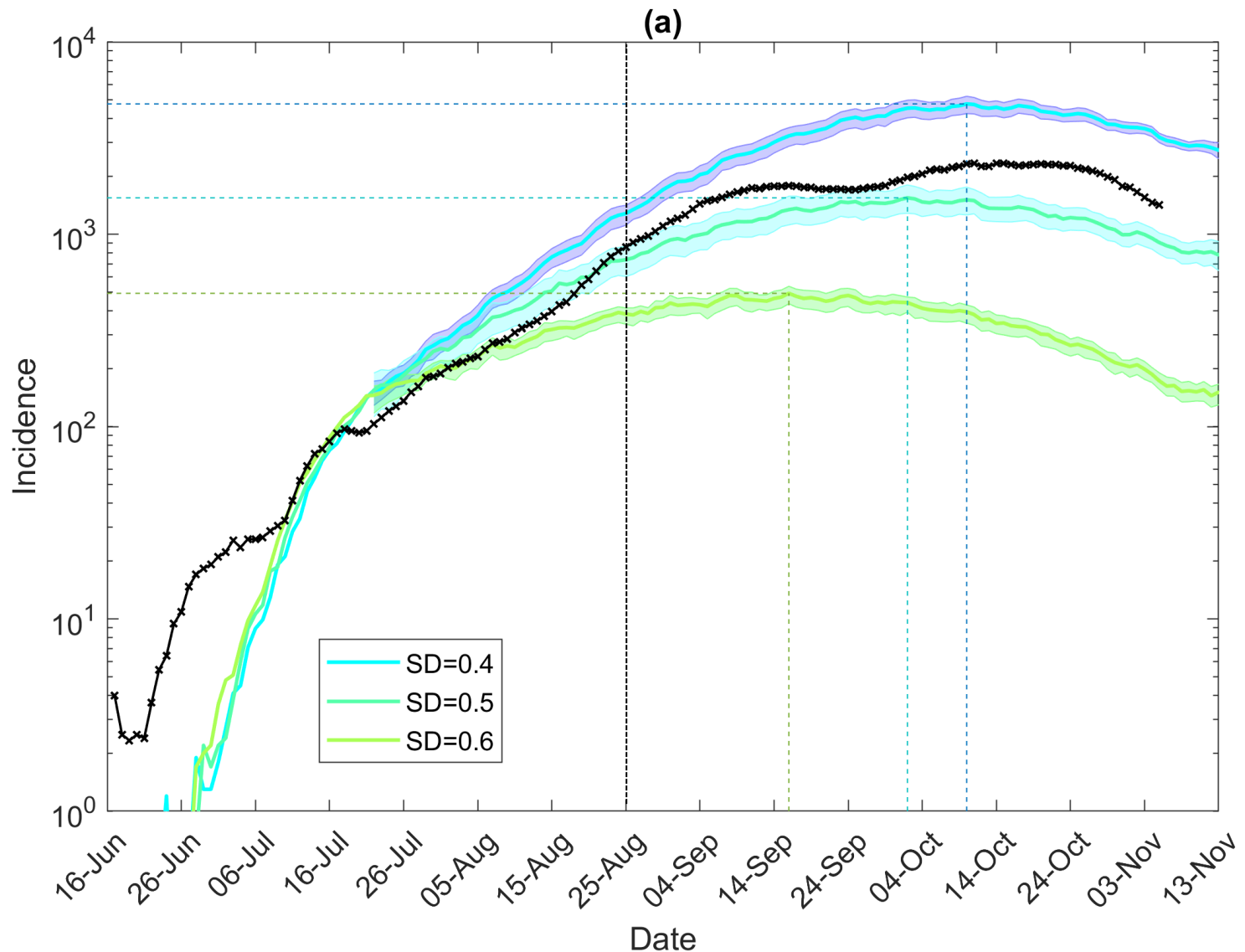


$$p_i^d(n) = (1 - V E_i^d) \sigma_{a|c} p_i(n)$$



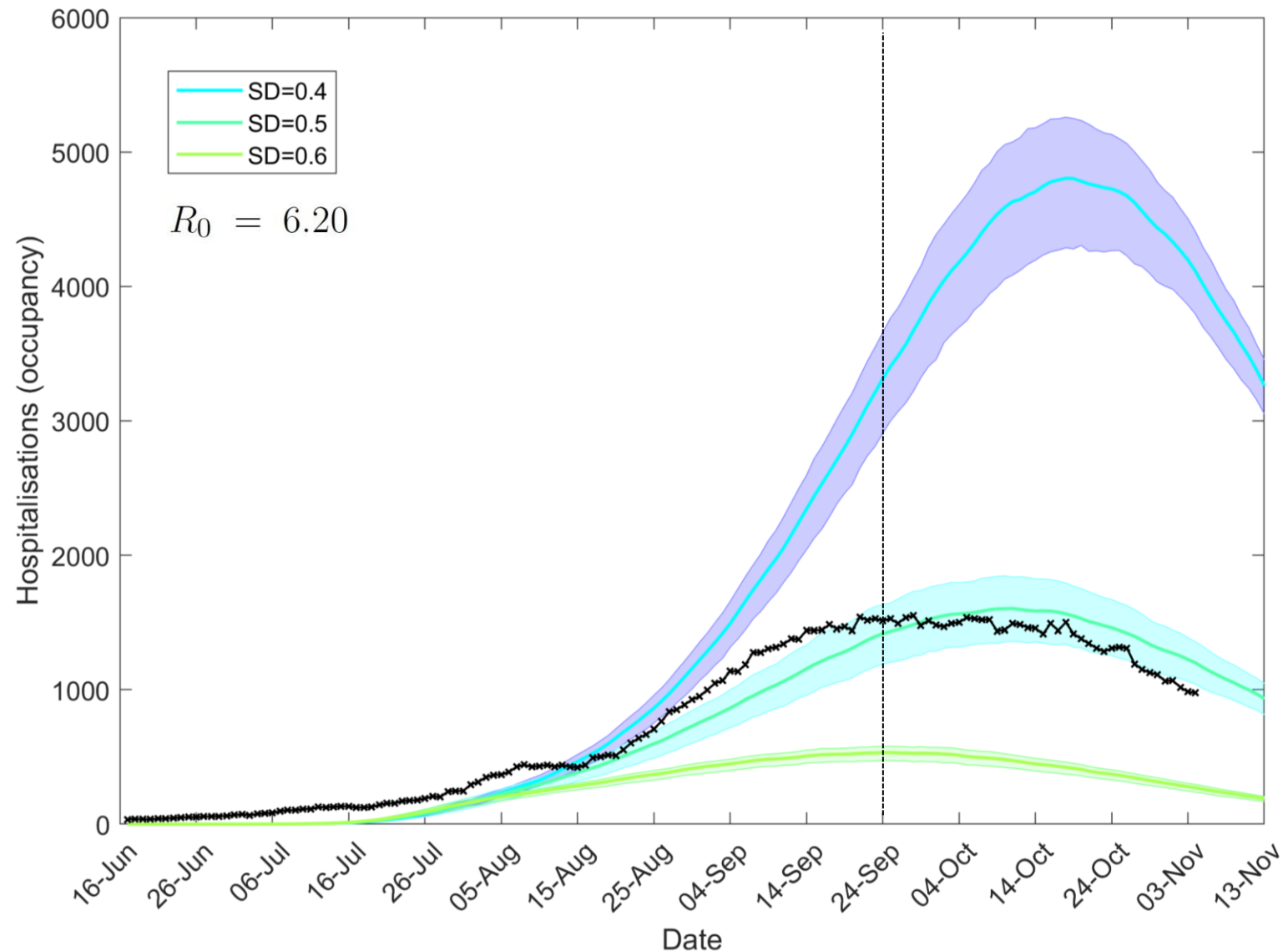
The Delta variant: scenarios across Australia (25 August → 5 November 2021)

$$R_0 = 6.20$$



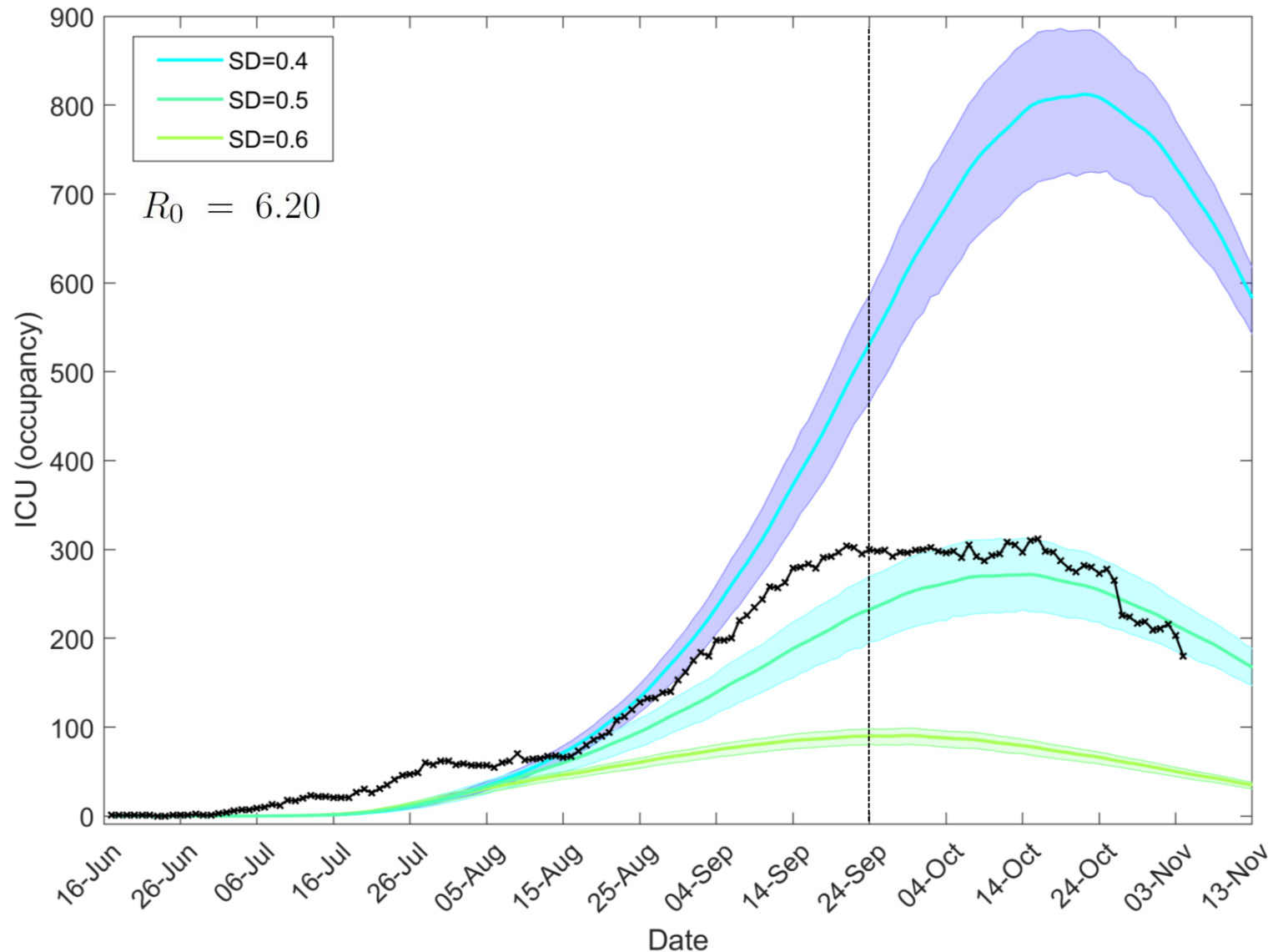


Hospitalisations (occupancy): a threefold reduction for 10% increase in SD



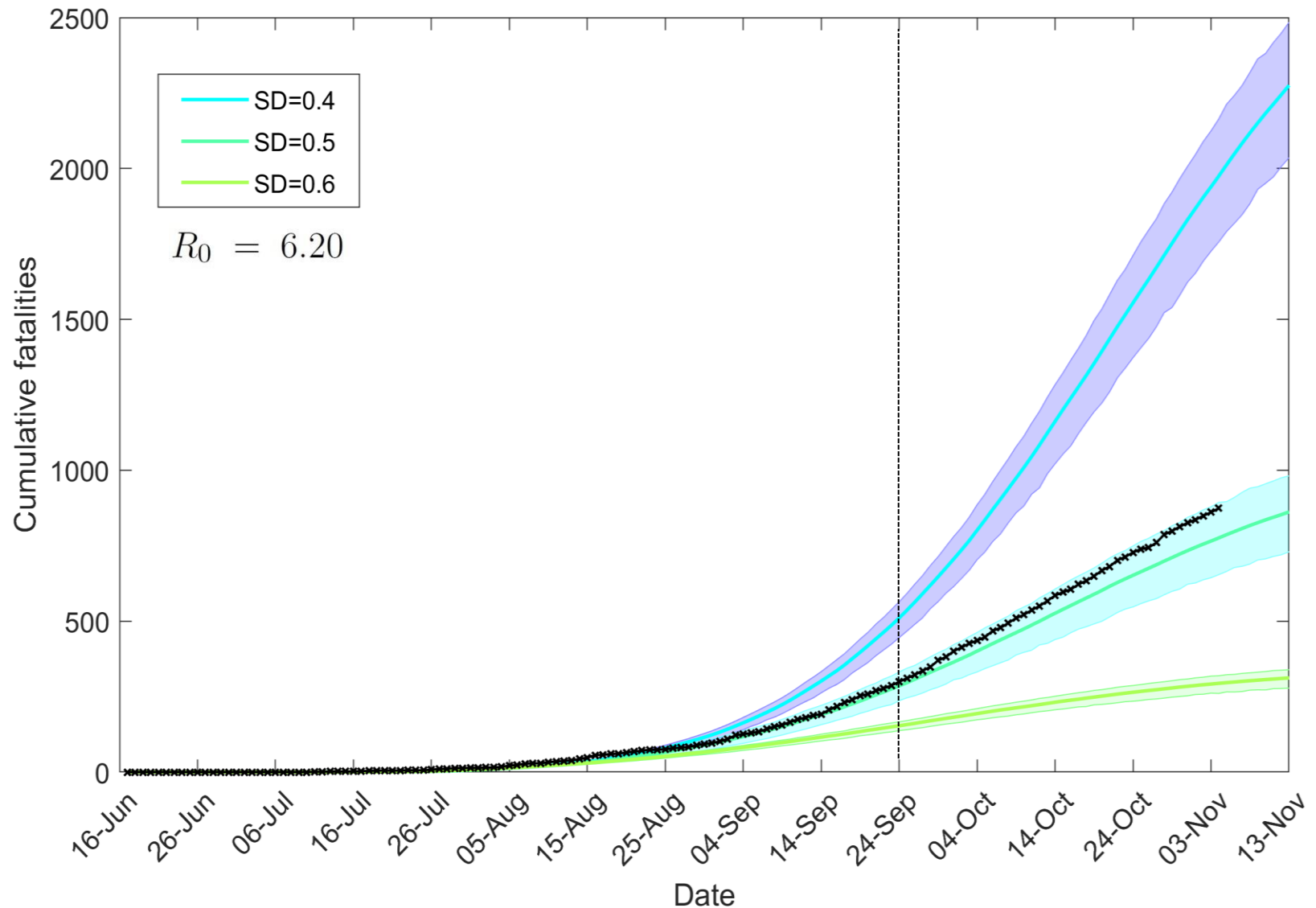


ICU (occupancy): a threefold reduction for 10% increase in SD

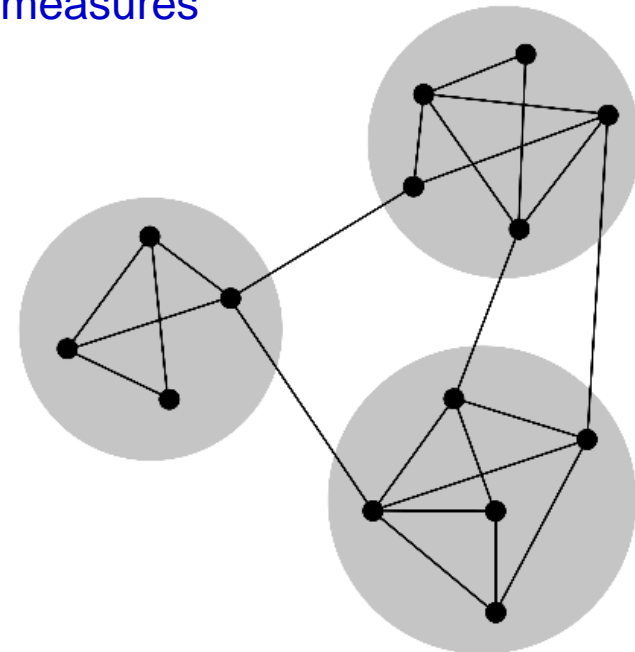




Fatalities (cumulative): a two-fold reduction for 10% increase in SD



- tipping points in social distancing (SD) compliance
- highly-transmissible variants strongly amplify small changes in SD compliance
- equity of vaccination targets: must be met for all population subgroups
- vaccination efficacy diminishes over time
- vaccine uptake and SD levels are uneven across demographics
- capacity limits of testing, tracing, isolation, quarantine measures
- declining compliance with SD
- multiple waves (superposition and heterogeneity)



➤ Strengths:

- individual-based rather than aggregate focus
- age-dependent epidemic characteristics
- geospatial accuracy and cross-jurisdictional impact
- nonlinearity: superposition of multiple waves
- time-dependent and context-dependent interventions (NPIs and vaccination)
- counter-factual analysis (“what-if” scenarios: delays, scale, scope)
- critical phenomena analysis

➤ Weaknesses:

- need to calibrate multiple parameters
- reliance on high-performance computing

- feedback from genomics
- in-hospital transmissions
- holidays, school terms, annual leaves, etc.
- maritime traffic (cruise ships)
- friendship networks
- contact tracing and large-scale testing capacity
- in-hotel quarantine
- occupation-based (sector-based) analysis → refined exit strategies
- seasonal effects
- GTAP, TAP (COVID-19 specific)
- local “lockdowns” (area quarantine)

December 14, 2021

Software

Open Access

AMTraC-19 (v7.7d) Source Code: Agent-based Model of Transmission and Control of the COVID-19 pandemic in Australia

 Chang, Sheryl L.;  Harding, Nathan;  Zachreson, Cameron;  Cliff, Oliver M.;  Prokopenko, Mikhail

The software implements an agent-based model for a fine-grained computational simulation of the COVID-19 pandemic in Australia. This model is calibrated to reproduce several features of COVID-19 transmission, including its age-dependent epidemiological characteristics. The individual-based epidemiological model accounts for mobility (worker and student commuting) patterns and human interactions derived from the Australian census and other national data sources. The high-precision simulation comprises approximately 24 million stochastically generated software agents and traces various scenarios of the COVID-19 pandemic in Australia. The software has been used to evaluate various intervention strategies, including (1) non-pharmaceutical interventions, such as restrictions on international air travel, case isolation, home quarantine, school closures, and stay-at-home restrictions with varying levels of compliance (i.e., "social distancing"), and (2) pharmaceutical interventions, such as pre-pandemic vaccination phase and progressive vaccination rollout.

The paper describing the model and the scenarios investigated with AMTraC-19 (v7.7d):

S. L. Chang, C. Zachreson, O. M. Cliff, M. Prokopenko, [Simulating transmission scenarios of the Delta variant of SARS-CoV-2 in Australia](#), *Frontiers in Public Health*, 10, 10.3389/fpubh.2022.823043, 2022.

Please cite it, as well as other publications referenced below, when using the software.


The dataset generated during this study is also available on Zenodo:

S. L. Chang, O. M. Cliff, C. Zachreson & M. Prokopenko. (2021). AMTraC-19 (v7.7d) Dataset: Simulating transmission scenarios of the Delta variant of SARS-CoV-2 in Australia (Version v1) [Data set]. Zenodo. <https://doi.org/10.5281/zenodo.5726241>

256

 views

8

 downloads[See more details...](#)

Indexed in

OpenAIRE

Publication date:

December 14, 2021

DOI:DOI [10.5281/zenodo.5778218](https://doi.org/10.5281/zenodo.5778218)**Keyword(s):**

computational epidemiology

COVID-19

SARS-CoV-2

agent-based model

pandemic model

discrete-time simulation

social distancing

vaccination

pandemic intervention

License (for files): GNU General Public License v2.0 or later



THE UNIVERSITY OF
SYDNEY

AMTraC-19 team



- S. Cauchemez, A. Bhattarai, T. L. Marchbanks, R. P. Fagan, S. Ostroff, N. M. Ferguson, D. Swerdlow; Pennsylvania H1N1 Working Group, Role of social networks in shaping disease transmission during a community outbreak of 2009 H1N1 pandemic influenza, *PNAS*, 108, 2825–2830, 2011.
- O. M. Cliff, N. Harding, M. Piraveenan, E. Erten, M. Gambhir, M. Prokopenko, Investigating spatiotemporal dynamics and synchrony of influenza epidemics in Australia: An agent-based modelling approach, *Simulation Modelling Practice and Theory*, 87, 412-431, 2018.
- K. M. Fair, C. Zachreson, M. Prokopenko, Creating a surrogate commuter network from Australian Bureau of Statistics census data, *Scientific Data*, 6, 150, 2019.
- T. C. Germann, K. Kadau, I. M. Longini Jr., C. A. Macken, Mitigation strategies for pandemic influenza in the United States, *PNAS*, 103, 5935–5940, 2006.
- N. Harding, R. E. Spinney, M. Prokopenko, Phase transitions in spatial connectivity during influenza pandemics, *Entropy*, 22(2), 133, 2020.
- K. Kadau, T. C. Germann, P. Lomdahl, Large-Scale Molecular-Dynamics Simulation of 19 Billion Particles, *International Journal of Modern Physics C*, 27(15): 193-201, 2004.
- C. Viboud, O. N. Bjørnstad, D. L. Smith, L. Simonsen, M. A. Miller, B.T. Grenfell, Synchrony, waves, and spatial hierarchies in the spread of influenza, *Science*, 312(5772): 447–451, 2006.
- C. Zachreson, K. M. Fair, O. M. Cliff, N. Harding, M. Piraveenan, M. Prokopenko, Urbanization affects peak timing, prevalence, and bimodality of influenza pandemics in Australia: Results of a census-calibrated model, *Science Advances*, 4(12), eaau5294, 2018.
- C. Zachreson, K. M. Fair, N. Harding, M. Prokopenko, Interfering with influenza: nonlinear coupling of reactive and static mitigation strategies, *Journal of Royal Society Interface*, 17(165): 20190728, 2020.
- S. L. Chang, N. Harding, C. Zachreson, O. M. Cliff, M. Prokopenko, Modelling transmission and control of the COVID-19 pandemic in Australia, *Nature Communications*, 11, 5710, 2020.
- C. Zachreson, S. L. Chang, O. M. Cliff, M. Prokopenko, How will mass-vaccination change COVID-19 lockdown requirements in Australia? *The Lancet Regional Health – Western Pacific*, 14: 100224, 2021.
- S. L. Chang, O. M. Cliff, C. Zachreson, M. Prokopenko, Simulating Transmission Scenarios of the Delta Variant of SARS-CoV-2 in Australia, *Frontiers in Public Health*, 10, 10.3389/fpubh.2022.823043, 2022.